

Alma Mater Studiorum Università di Bologna
Archivio istituzionale della ricerca

The challenging playground of astrochemistry: An integrated rotational spectroscopy-quantum chemistry strategy

This is the final peer-reviewed author's accepted manuscript (postprint) of the following publication:

Published Version:

Puzzarini C., Barone V. (2020). The challenging playground of astrochemistry: An integrated rotational spectroscopy-quantum chemistry strategy. PHYSICAL CHEMISTRY CHEMICAL PHYSICS, 22(12), 6507-6523 [10.1039/d0cp00561d].

Availability:

This version is available at: <https://hdl.handle.net/11585/783303> since: 2020-12-04

Published:

DOI: <http://doi.org/10.1039/d0cp00561d>

Terms of use:

Some rights reserved. The terms and conditions for the reuse of this version of the manuscript are specified in the publishing policy. For all terms of use and more information see the publisher's website.

This item was downloaded from IRIS Università di Bologna (<https://cris.unibo.it/>).
When citing, please refer to the published version.

(Article begins on next page)

This is the final peer-reviewed accepted manuscript of:

C. Puzzarini, V. Barone. The challenging playground of astrochemistry: an integrated rotational spectroscopy – quantum chemistry strategy. Phys. Chem. Chem. Phys. 22, 6507 (2020)

The final published version is available online at:

<https://doi.org/10.1039/D0CP00561D>

Terms of use:

Some rights reserved. The terms and conditions for the reuse of this version of the manuscript are specified in the publishing policy. For all terms of use and more information see the publisher's website.

This item was downloaded from IRIS Università di Bologna (<https://cris.unibo.it/>)

When citing, please refer to the published version.

Cite this: DOI: 10.1039/xxxxxxxxxx

The challenging playground of astrochemistry: an integrated rotational spectroscopy - quantum chemistry strategy

Cristina Puzzarini^{*a} and Vincenzo Barone^b

Received Date

Accepted Date

DOI: 10.1039/xxxxxxxxxx

www.rsc.org/journalname

While it is now well demonstrated that the interstellar medium (ISM) is characterized by a diverse and complex chemistry, a significant number of features in radioastronomical spectra are still unassigned and call for new laboratory efforts, which are increasingly based on integrated experimental and computational strategies. In parallel, the identification of an increasing number of molecules containing more than five atoms and at least one carbon atom (the so-called “interstellar” complex organic molecules), which can play a relevant role in the chemistry of life, raises the additional issue of how these species can be produced in the typical harsh conditions of the ISM. On these grounds, this perspective aims to present an integrated rotational spectroscopy - quantum chemistry approach for supporting radioastronomical observations and a computational strategy for contributing to the elucidation of chemical reactivity in the interstellar space.

1 Introduction

Since the discovery of the interstellar gas¹ and dust², it has been thought that the extreme conditions of the interstellar medium (ISM, with temperatures ranging between 10 and 100 K, very low density and ionizing radiations) could only allow the presence of atoms. It was only when radioastronomy took hold –nearly fifty years ago– that it became clear that the ISM was home to a large panel of interesting polyatomic (both organic and inorganic) molecules. Particularly fascinating amongst the molecules discovered in the ISM are the so-called “interstellar complex organic molecules” (iCOMs)³, which are –by definition– molecules containing more than 5 atoms and including at least one carbon atom. Examples are glycoaldehyde⁴, acetamide⁵, aminoacetonitrile^{6,7}, and methyloxirane⁸. Generally, iCOMs combine multiple functional groups illustrative of the rich chemistry of the ISM. The discovery of all of these polyatomic species has led to the emergence of the field of astrochemistry, an interdisciplinary and multifaceted discipline at the interface of chemistry, physics, and astronomy, which encompasses astronomical observations and modeling, as well as theoretical and experimental laboratory investigations⁹. While the evidence for molecular complexity in the universe is now undisputed, there is still much to be understood about the formation of molecules in the typically cold and (largely) collision free environment of the ISM.

In the field of astrochemistry, molecular spectroscopy plays

a central role (see, e.g., 3,9–11). Because of the tremendous distances involved, there is no chance to perform direct experiments on astrochemical processes, and detection via interaction of molecules with radiation is the only viable route of investigation^{9,11,12}. The astronomical observation of the spectroscopic features of a given molecule is the definitive, unequivocal proof of its presence in the astronomical environment under consideration (e.g. refs. 8,13–19). The overwhelming majority of gas-phase chemical species in the cosmos have been discovered via their rotational signatures. Indeed, the systematic observation of a given astronomical source leads to line surveys that in principle deliver a nearly complete census of the molecular content, with the exception of apolar molecules (which do not show rotational spectra). The assignment of these surveys allows for an unbiased picture of the chemical composition and also provides additional useful information such as temperature and density. Powerful astronomical facilities like ALMA (Atacama Large Millimeter Array) offer unprecedented resolution and sensitivity as well as frequency coverage, thus providing unique opportunities to extend our knowledge of the molecular inventory of the universe (see, e.g., ref. 14). On the other hand, sensitivity and resolution increase the number of lines that ultimately must be assigned, thus requiring a massive parallel laboratory effort. Indeed, the complexity of radioastronomical surveys requires the accurate knowledge of the spectroscopic features of potential iCOMs, which can be obtained only from laboratory studies. Although more than 200 species have been detected in space, these spectral line surveys continue to reveal hundreds of features not assignable to transitions of molecules already characterized by laboratory in-

^a Dipartimento di Chimica “Giacomo Ciamician”, University of Bologna, via F. Selmi 2, I-40126 Bologna, Italy. E-mail: cristina.puzzarini@unibo.it

^b Scuola Normale Superiore, Piazza dei Cavalieri 7, I-56126, Pisa, Italy.

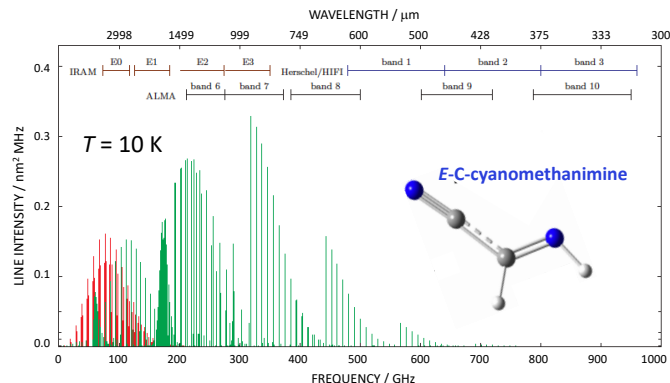


Fig. 1 Simulated rotational spectrum of *E*-C-cyanomethanimine at $T = 10$ K based on the global fit of ref. 23. In red: *a*-type transitions, in green: *b*-type transitions.

vestigations.

The main reason why a number of radioastronomical features is still not assigned is thus the lack of the corresponding spectroscopic information. Within this general problem, two major issues can be pinpointed. If experimental information is completely missing, the experimental work is usually first of all carried out at low frequency, i.e., in the centimeter-wave region, using a Fourier Transform Microwave (FTMW) spectrometer^{20,21} and then the study is extended in the millimeter/submillimeter-wave frequency range²². The second possible scenario is that rotational transitions in the low frequency regime are available. Since extrapolations from low-frequency laboratory measurements might provide inaccurate and/or unreliable predictions for higher frequency regimes (millimeter/submillimeter-wave region), ad hoc laboratory investigations of the rotational spectra are required, the final outcome being the accurate knowledge of the rotational spectrum in all, or most of, working range of ALMA (84–950 GHz). Because of the high sensitivity and resolution of the unbiased spectral surveys that are currently obtained, especially, from interferometric radioastronomy, rotational transition frequencies must be known with an accuracy preferably better than 100 kHz. Figure 1 shows the simulated rotational spectrum of *E*-C-cyanomethanimine, at the temperature of 10 K, based on the work of ref. 23, and it allows us to point out that, even at such a low temperature, the most intense transitions can lie in the submillimeter-wave frequency range. Therefore, identifying or not a molecule in the ISM can be very sensitive to the availability of laboratory measurements in the millimeter/submillimeter-wave region. Indeed, predictions based on extrapolations from low-frequency data not only can be affected by uncertainties larger than 100 kHz (even of the order of a few MHz), but also can be off by more than the predicted errors.

The detection of an increasing number of molecules, often showing some degree of complexity, has given rise to the challenge of understanding how these could be produced. This branch of Astrochemistry thus aims to propose and validate formation pathways that are feasible in the extreme conditions of the ISM, also providing kinetic information to be then used for building chemical models able to explain the observed abundances.

Because of difficulties in mimicking the extreme conditions that characterize the ISM in the laboratory, accurate state-of-the-art computational approaches play a fundamental role in analyzing feasible reaction mechanisms. Indeed, modern quantum chemistry is an extremely powerful tool that can assist experiment by providing accurate predictions of spectroscopic parameters (e.g. refs. 24–32) and can also accurately predict the kinetics associated with postulated mechanisms for reactive systems. As a result, quantum-chemical calculations are increasingly exploited for these purposes (e.g. refs. 33–38). Reaction schemes taking into account all relevant pathways need to be formulated, thus requiring the identification of all intermediate species, from reactants to products, as well as the transition states connecting them. In practical terms, accurate electronic structure calculations are carried out for every chemical species involved in the mechanism in order to obtain structure, energies, spectroscopic properties and from them thermochemical data (e.g., ref. 33). The latter can then be fed into a suitable tool to compute the outcome of the reactions through use of master-equation models³⁹ and suitable techniques to determine the kinetics of the elementary processes involved in the reaction scheme (see, e.g., refs. 33,35,36,40,41). Furthermore, explicit dynamical calculations are needed whenever transition state theory and its more advanced extensions⁴² break down (see, e.g. ref. 43). Overall, computational approaches are actually able to simulate abundances in agreement with astronomical observations (see, e.g., refs. 40,44).

As mentioned above, there is much to be understood about the chemical evolution in interstellar spaces. Initially, in the early seventies, molecular synthesis through gas-phase ion-neutral reactions was proposed and successfully rationalized the molecular abundances observed in interstellar clouds. Later, the importance of neutral-neutral reactions was recognized, even in low-temperature conditions. However, as observational capabilities advanced over the past decade, iCOMs began to be detected in regions where gas-phase reactions did not contribute significantly to chemical processing (see, e.g., refs. 45,46). Several studies led to the recognition that chemical reactions occurring on the surface of (icy) dust grains were critical sources of molecules and that these grains, which could effectively serve as both catalyst and a sink for the deposition of chemical energy, play an important role in the chemistry of space^{46,47}. Currently, it is clear that synthesis can proceed via surface chemistry or in the gas phase (see, e.g., refs. 48,49); however, the mechanisms leading to iCOMs are often still object of debate.

In this perspective, two astrochemical challenges will be addressed: the detection of iCOMs in the ISM and their possible formation routes. For the former, we will focus on laboratory studies that can enable the detection of a chemical species in space, with special attention to rotational spectroscopy and the interplay of experiment and theory. For the second challenge, we will only consider accurate quantum-chemical approaches for investigating gas-phase formation pathways of iCOMs. While there is an extensive literature on both topics, we will focus on the results obtained in our laboratories.

of the experimental spectrum.

The prediction and analysis of rotational spectra are usually carried out in terms of an effective rotational Hamiltonian, which incorporates pure rotational and centrifugal-distorsion contributions and describes the rotational energy levels for a given vibrational state, with the ground state usually being the one of interest. While a complete treatment can be found in the literature (see, for example, refs. 60,61), the key aspects will be briefly summarized in the following.

Within the semi-rigid rotor approximation, the basic rotational Hamiltonian can be written as

$$H_{\text{rot}} = H_{\text{rot}} + H_{\text{qcd}} + H_{\text{scd}} + \dots, \quad (1)$$

where H_{qcd} and H_{scd} are the quartic and sextic centrifugal terms, respectively, and the dots refer to the possibility of including either higher-order centrifugal contributions or other terms, such as those due to hyperfine interactions^{26,29,60}. H_{rot} is the rigid-rotor Hamiltonian, which is defined as:

$$H_{\text{rot}} = \sum_{\tau} \mathbf{B}_{\tau}^{\text{eq}} \mathbf{J}_{\tau}^2, \quad (2)$$

where $\mathbf{B}_{\tau}^{\text{eq}}$ is defined as follows:

$$\mathbf{B}_{\tau}^{\text{eq}} = \frac{\hbar^2}{2hcI_{\tau\tau}^{\text{eq}}}, \quad (3)$$

with τ referring to the inertial axis, and $I_{\tau\tau}^{\text{eq}}$ denoting the τ -th diagonal element of the equilibrium inertia tensor \mathbf{I}^{eq} . Since the latter only depends on equilibrium structure and isotopic masses, from a computational point of view, the equilibrium rotational constants are straightforwardly obtained from the geometry optimization.

Even if the equilibrium contribution to rotational constants is the most important, the effect of molecular vibrations cannot be neglected when aiming at a quantitative description of rotational spectra. The term describing the dependence of the rotational constants on the vibrational quantum numbers should be incorporated, with the effective rotational constants thus replacing the equilibrium ones. Effects of vibrations on rotational motion can be conveniently described by means of vibrational perturbation theory (VPT), and we refer the reader to, for example, refs. 61,62 for a detailed treatment. While there are no corrections at the first order in VPT, at the second order (VPT2) the expression for a generic rotational constant is given by⁶³:

$$\mathbf{B}_{\tau}^{\text{v}} = \mathbf{B}_{\tau}^{\text{eq}} - \sum_{i=1}^N \alpha_{i,\tau} \left(v_i + \frac{d_i}{2} \right), \quad (4)$$

where the superscript v denotes the vibrational state and the sum runs over all fundamental vibrational modes i , with v_i being the corresponding quantum number and d_i its degeneracy order. The $\alpha_{i,\tau}$'s are denoted as vibration-rotation interaction constants and, from a computational point of view, their evaluation requires anharmonic force field calculations. For the vibrational ground

state, eq. (4) becomes:

$$\mathbf{B}_{\tau}^0 = \mathbf{B}_{\tau}^{\text{eq}} - \frac{1}{2} \sum_{i=1}^N \alpha_{i,\tau} = \mathbf{B}_{\tau}^{\text{eq}} + \Delta B_{\text{vib},\tau}. \quad (5)$$

In passing we note that an additional contribution to equilibrium rotational constants is the electronic correction, which is –in most cases– negligible. The evaluation of this term requires the diagonal elements of the rotational g -factor together with the electron and proton mass ratio^{64–66}.

The quartic centrifugal-distorsion Hamiltonian is defined as

$$H_{\text{qcd}} = \frac{1}{4} \sum_{\tau\eta\zeta\rho} \tau_{\tau\eta\zeta\rho} \mathbf{J}_{\tau} \mathbf{J}_{\eta} \mathbf{J}_{\zeta} \mathbf{J}_{\rho}, \quad (6)$$

where the tensor $\tau_{\tau\eta\zeta\rho}$ depends only on the harmonic part of the potential energy surface (PES). To obtain the quartic centrifugal distortion parameters entering the most suitable effective Hamiltonian, further contact transformations with purely rotational operators (thus diagonal in the vibrational quantum numbers) are then required. An analogous expression can be written for the sextic centrifugal-distortion term H_{scd} , and the computation of the corresponding sextic centrifugal-distortion constants involves harmonic, anharmonic, and Coriolis perturbation terms. Therefore, from a computational point of view, quartic and sextic centrifugal distortion constants can be obtained as byproducts of harmonic and anharmonic force field computations, respectively. To relate the experimental parameters to combinations of $\tau_{\tau\eta\zeta\rho}$ ($\tau_{\tau\eta\zeta\rho\epsilon\iota}$ in the case of sextics), it is necessary to further, completely reduce the Hamiltonian. Different results are then obtained depending on the reduction chosen. The reader is referred, for example, to refs. 61,62,67.

In the framework of rotational spectroscopy, in order to obtain quantitative spectral prediction/analysis, computations of spectroscopic parameters need to be very accurate. The key point to reach this goal is to greatly reduce the errors associated to quantum-chemical calculations. To fulfil this task, the best option is to rely on composite schemes, which are approaches that evaluate the contributions important to reach high accuracy at the best possible level and combine them through the additivity approximation (see, e.g., refs. 26,28,29,66,71–81).

The starting point is an accurate and reliable description of the equilibrium structure, which is defined as a minimum on the Born-Oppenheimer (BO) PES. While in the presence of strong static correlation effects multireference treatments are unavoidable, in the overwhelming majority of cases, the methods of choice are composite schemes based on coupled-cluster techniques including single and double excitations and a perturbative treatment of triples, CCSD(T)⁸², and that account for extrapolation to the complete basis set (CBS) and core-valence (CV) correlation effects (i.e, the so-called CCSD(T)/CBS+CV scheme⁷⁴). These models are able to provide equilibrium structures with an accuracy of 0.001-0.002 Å for bond lengths and 0.05-0.1 degrees for angles. However, composite approaches entirely based on CCSD(T) are computationally expensive. To overcome the computational cost, the so-called “cheap” composite approach has been introduced⁸³, which is based on frozen-core CCSD(T)

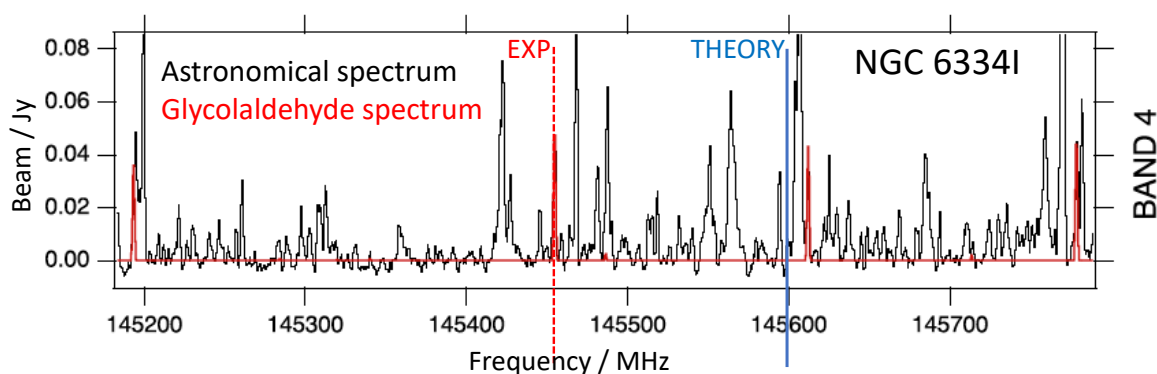


Fig. 3 Simulated rotational spectrum of glycolaldehyde ($\text{HC(O)CH}_2\text{OH}$) plotted in red (data from the Cologne database^{68,69}) over ALMA observations (band 4) of NGC 6334I MM1 plotted in black.⁷⁰ The comparison between experiment and theory for the $J = 22_{7,15} \leftarrow 22_{6,16}$ rotational transition of glycolaldehyde is also reported.

computations in conjunction with a triple-zeta quality basis set, but employs Møller-Plesset perturbation theory to second order (MP2)⁸⁴ to incorporate corrections due to the extrapolation to the CBS limit and CV contributions. Various composite approaches have been developed by research groups all around the world. Even if the following list is not exhaustive, the reader is referred to refs. 72–74,83,85–89. In passing we note that composite schemes can also be applied to the accurate computation of harmonic force fields (see, for example, refs. 78,90–93).

Based on two recent statistical studies involving molecular species only containing first-row atoms⁶⁶ and on molecules also bearing second-row elements⁹⁴, equilibrium rotational constants can be predicted with a standard deviation smaller than 0.1% when geometries are optimized at the CCSD(T)/CBS+CV+fT+fQ level, which accounts –in addition to CBS and CV contributions– for corrections due to the full treatment of triples (fT) and quadruples (fQ). Relativistic and (non-)diagonal Born-Oppenheimer contributions might also be required in the most accurate computations (see, e.g., refs. 95–98). However, the more affordable CCSD(T)/CBS+CV scheme usually provides similar accuracy (exceptions being, e.g., conjugated radicals⁹⁹). Once moving from equilibrium to vibrational ground-state rotational constants, in order to keep high accuracy, it is mandatory to include the vibrational corrections according to eq. (5)^{26,66,100–102}, with the latter being efficiently computed already at the density functional theory (DFT) level^{17,103–105}, provided that proper hybrid (e.g. B3LYP^{106–108}) or, better, double-hybrid (e.g. B2PLYP^{109,110}) functionals are used in conjunction with at least partially augmented triple-zeta basis set and, when needed, semi-empirical treatment of dispersion interactions (e.g. DFT-D3 scheme¹¹¹).

According to the literature on this topic (see, e.g., refs. 17, 66,88,94,102,112–115), best-estimated spectroscopic parameters can lead to the prediction of rotational transitions with a relative accuracy better than 0.1% in the centimeter/millimeter-wave region, with this upper limit increasing up to 0.15–0.2% in the far-infrared region. This means that the best computed parameters can predict rotational frequencies at 150 GHz with an uncertainty of about 150 MHz. An example is provided by Figure 3, which

shows the comparison between experiment and theory for the $J = 22_{7,15} \leftarrow 22_{6,16}$ rotational transition of glycolaldehyde. This figure further points out that state-of-the-art quantum-chemical computations are able to guide astronomical searches and/or assignment only when astronomical spectra are characterized by a limited number of features, very well separated one from the other, but not in the case of congested spectral line surveys as those obtained with ALMA. On the contrary, computations are suitable for guiding experiment in the laboratory.

The last note concerns the identification of the conformational minima of flexible molecules. The usual strategy relies on relaxed scans of the PES along the dihedral angles. However, for complex systems, two-stage stochastic methods¹¹⁶ can be employed.

2.1.1 Laboratory measurements

Rotational transitions lie in the range of <1 GHz to 3 THz⁶⁰, with very light molecules covering almost all this range and the spectral distribution of heavy compounds being “squeezed” at very low frequency^{11,22}, as shown in Figure 4. Indeed, rotational transition frequencies are mainly determined by the rotational constants, whose values range from less than 1 GHz for large molecules up to ~1300 GHz for a molecule as small as HD. Therefore, the millimeter and submillimeter wavelength regions are those of interest to detect small to medium-sized molecules, while observations in the centimeter-wave regime allow the identification of medium-sized to larger species.* Figure 4 serves as an example: the rotational spectrum of a molecule as light as HCN is spread over the 0 to 2 THz range, while that of HC_3N (at $T = 100$ K) drops down to zero intensity already at 180 GHz. Furthermore, because of the density of rotational states, the overall intensity of rotational lines is decreased.

While we refer interested readers to refs. 22,117,118 (and references therein) for thorough descriptions of the rotational spectroscopic techniques, a rough classification is given in the follow-

*The centimeter-wave region covers approximately the range 3–30 GHz (wavelength, λ : 1 dm–1 cm), while the millimeter-wave region corresponds to the 30–300 GHz range (λ : 1 cm–1 mm). The latter is followed at higher frequencies by the submillimeter-wave region (also denoted far-infrared region), which covers the largest frequency range, i.e., from 300 GHz up to 3 THz (λ : 1 mm–0.1 mm).

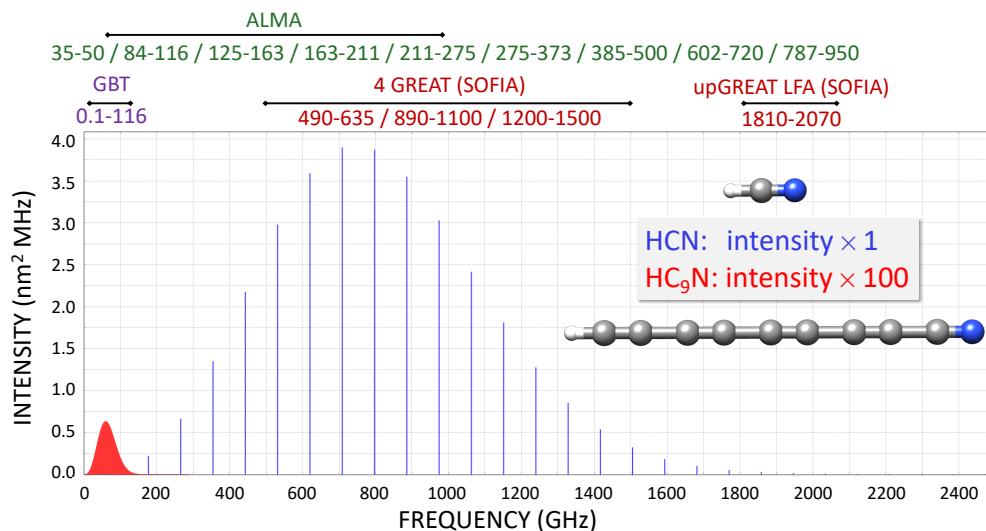


Fig. 4 Simulated rotational spectra of HCN and HC₉N (data from the Cologne database^{68,69}) at $T = 100$ K. Working frequency ranges (in GHz) of the GBT, ALMA bands (from left to right: band 1, and bands 3 to 10), the GREAT receiver bands (three of the 4 GREAT bands; from left to right: Herschel/HIFI Band 1, Herschel/HIFI Band 4, GREAT L1; the GREAT M channel –2490–2590 GHz– is not shown) and the upGREAT low frequency array (LFA) are also displayed.

ing. For rotational spectrometers, two main categories can be identified: those working in the time domain and, thus, based on the Fourier-transform (FT) technique^{20,21} and those working in the frequency domain and, thus, performing continuous-wave (CW) measurements (see, e.g., refs. 22,119–122 and references therein). The former instrumentation usually works in the centimeter-wave region (with a few exception up to 300 GHz; see, e.g., refs. 123,124), with a improvement being the employment of chirped-pulse excitation, which allows broadband measurements¹²⁵. Conversely, CW spectrometers can work in the entire frequency region, and are mostly used in the millimeter- and submillimeter-wave frequency ranges. In Figure 4, the working ranges of the Green Bank telescope (GBT), the ALMA bands[†], and the GREAT receiver bands (onboard the Stratospheric Observatory for Infrared Astronomy, SOFIA) are reported. This allows us to point out that laboratory measurements are important over the entire microwave region.

2.2 Formation pathways of iCOMs

As mentioned in the Introduction, accurate state-of-the-art computational approaches play a key role in evaluating formation pathways that can occur in the extreme conditions typical of the ISM. Different astrochemical databases (like KIDA¹²⁶) collect kinetic parameters for thousands of reactions involving hundreds of chemical species. However, much of the information in these models is missing, approximated, or inadequate for other reasons. Since kinetic models are such that products of each elementary process are the reactants of the successive step, a small error in the thermochemical or kinetic data may propagate across the reaction network and thereby destroying its fidelity.

The prediction of accurate reaction rate constants is very chal-

lenging also for theoretical chemistry, especially at low temperature, because the rates of reactions are extremely sensitive to factors such as barrier heights and quantum tunneling effects. This implies that, before proceeding with the kinetic analysis, the energetics of the reactive PES needs to be accurately determined, and it is on this issue that we focus our attention. The key steps of our strategy in this respect will be briefly summarized in the following.

The starting point is an accurate sampling of the reactive PES to locate stationary points (minima and transition states) and, for this purpose, we rely on DFT. Since the use of double-hybrid functionals can be expensive, especially in connection with energy derivatives, a preliminary scan of the PES is carried out by using the cheaper B3LYP hybrid functional^{106,107} in conjunction with a double-zeta quality basis set. Noted is that this level of theory is similar to that employed for geometry optimizations in widely used composite methods (e.g. CBS-QB3^{127,128}). Subsequently, B3LYP stationary points are refined by means of the double-hybrid B2PLYP functional¹⁰⁹ in conjunction with a partially augmented triple-zeta quality basis set¹²⁹. In all cases, to correctly describe the long-range London dispersion interactions, Grimme's DFT-D3 scheme¹¹¹ employing the Becke-Johnson (BJ) damping function¹³⁰ is exploited. While the accuracy of B2PLYP-D3(BJ) geometries is generally more than adequate (see, e.g., ref. 131 and references therein), if required, their reliability and accuracy are checked with respect to composite schemes. From this first analysis of the PES, it is possible to identify the paths that are accessible at very low temperatures, i.e. those that only present submerged transition states.

The next point is the very accurate evaluation of the energy and other thermochemical properties for all stationary points of the selected paths. This task requires to employ composite quantum-chemical approaches. While a number of highly accurate schemes have been introduced (see, e.g., refs. 28,76,77,79–81,89,132),

[†] ALMA band 1 is still under construction.

our reference scheme is the HEAT protocol^{79,133,134}, which provides sub-kJ mol⁻¹ accuracy. Whenever possible (i.e. according to the dimension of the system under consideration), single-point energy calculations are performed using the following model:

$$E_{tot} = E_{\text{HF-SCF}}^{\infty} + \Delta E_{\text{CCSD(T)}}^{\infty} + \Delta E_{\text{CV}} + \Delta E_{\text{rT}} + \Delta E_{\text{rQ}} + \Delta E_{\text{REL}} + \Delta E_{\text{DBOC}}, \quad (7)$$

where $E_{\text{HF-SCF}}^{\infty}$ and $\Delta E_{\text{CCSD(T)}}^{\infty}$ denote the extrapolation to the CBS limit of the HF-SCF energy using the exponential formula by Feller⁷¹ and the CCSD(T) correlation energy (within frozen-core, fc, approximation) extrapolated to the CBS limit with the n^{-3} expression¹³⁵, respectively. The correlation-consistent cc-pVnZ basis sets¹³⁶ are employed in conjunction with these calculations, with $n=T, Q$ and 5 being usually chosen for the HF-SCF extrapolation, and $n=T$ and Q for the CCSD(T) correlation energy. The ΔE_{CV} term allows for incorporating the core-valence correlation correction, evaluated as energy difference between all-electron (ae) and fc CCSD(T) computations in the same basis, which is usually the cc-pCVTZ set¹³⁷. In a similar manner, corrections due to a full treatment of triples, ΔE_{rT} , and quadruples, ΔE_{rQ} , are computed as energy differences between CCSDT^{138–140} and CCSD(T) and between CCSDTQ¹⁴¹ and CCSDT (all within the fc approximation) employing the cc-pVTZ and cc-pVDZ basis sets, respectively. Since CCSDTQ calculations are computationally very expensive even in conjunction with a double-zeta basis set, the effect of quadruple excitations can be estimated using the CCSDT(Q) model^{142–144}. The diagonal Born-Oppenheimer correction^{145–148}, ΔE_{DBOC} , and the scalar relativistic contribution to the energy, ΔE_{REL} ,^{149,150} are also included. The former corrections are usually computed at the HF-SCF/aug-cc-pVnZ level¹⁵¹, with $n=D, T$, and the relativistic corrections are obtained at the ae-CCSD(T)/aug-cc-pCVnZ level ($n=D, T$) including the (one-electron) Darwin and mass-velocity terms.

While the approach introduced above can be employed for systems with less than 10 atoms or for selected, crucial stationary points requiring great accuracy, the variant only accounting for the extrapolation to the CBS limit and core-correlation contribution (i.e. CCSD(T)/CBS+CV) can be otherwise used, thus leading to energies that should be accurate to 1–2 kJ mol⁻¹. Less computationally demanding schemes, but still showing an accuracy comparable to that provided by CCSD(T)/CBS+CV, can be employed for larger systems. Among them, we resort to the so-called “cheap” composite approach¹⁵²:

$$E_{\text{cheap}} = E(\text{CCSD(T)}/\text{VTZ}) + \Delta E^{\text{CBS}}(\text{MP2}) + \Delta E_{\text{CV}}(\text{MP2}), \quad (8)$$

where, starting from the fc-CCSD(T)/cc-pVTZ level of theory, the corrections due to extrapolation to the CBS limit and CV effects are incorporated at the MP2 level. The cc-pVnZ, with $n=T, Q$, basis sets are used for the former correction, while the cc-pCVTZ set is employed for evaluating the CV contribution. Proper inclusion of diffuse functions can become mandatory when non-covalent interactions are involved¹⁵³.

A note on the quantum-chemical treatment of open-shell species is deserved because efficient reactions in the ISM often

involve radicals. Indeed, open-shell systems introduce additional problems related to spin contamination for unrestricted (U) approaches and to slow convergence of many-body contributions for restricted open-shell (RO) methodologies. In the case of doublet electronic states, the UCCSD(T) model fully removes the quartet contamination and generally leads to reasonable results¹⁵⁴. However, this is not sufficient in the presence of more significant spin contamination as is the case, for instance, of the CN radical. In such cases, full inclusion of triple excitations becomes mandatory and at this level restricted and unrestricted open-shell approaches tend to lead to equivalent results. However, a fully balanced model requires the inclusion of quadruple excitations, at least at a perturbative level. The situation is different for approaches rooted in the DFT¹⁵⁵. In particular, double-hybrid functionals usually deliver results of comparable accuracy for closed- and open-shell systems, thereby employing, in the second case, an unrestricted approach (which always leads to small spin contaminations¹⁵⁶). As will be shown in a specific example, the “cheap” scheme based on RO calculations performs well, even in the description of a reaction mechanism that involves the CN radical.

To incorporate zero-point vibrational energy (ZPE), the corresponding energy corrections are usually evaluated within the harmonic approximation. However, the accuracy of the composite approaches described above for electronic energies calls for evaluations of ZPEs beyond the harmonic approximation. In the framework of VPT2, a reformulation of the standard expressions allows for obtaining anharmonic ZPEs devoid of any kind of resonance⁷⁵. In ref. 157, the degeneracy-corrected PT2 approach (DCPT2) has been extended to a hybrid version (HD-CPT2), which also includes an automatic treatment of internal rotations through the hindered-rotor model, thus providing a fully black box model for both minima and transition states. Since soft degrees of freedom (e.g. hindered rotations or inversions) can be poorly described by perturbative approaches, whenever their coupling with other modes is negligible, they can be effectively treated by one-dimensional variational or quasi-variational approaches^{32,158}.

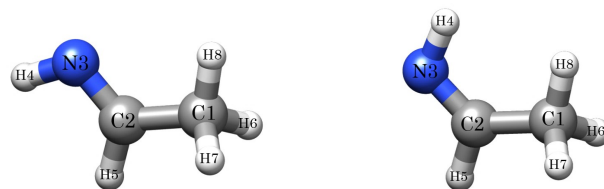


Fig. 5 Isomers of ethanimine: the most stable *E* form is displayed on the left, the *Z* isomer on the right (2.77 kJ mol⁻¹ higher in energy). They are separated by an energy barrier computed to be 115.7 kJ mol⁻¹.¹⁷

3 Results and Discussion: case studies

Some case studies have been selected in order to illustrate how the synergy between rotational spectroscopy and quantum chemistry can contribute to shed some light on astrochemical challenges. As already mentioned, the focus is on prebiotic iCOMs. Starting from spectroscopic studies aiming at supporting detections in the ISM, we will then move to the investigation of forma-

tion mechanisms.

3.1 Prebiotic iCOMs: the case of ethanimine

The first application of the VMS-ROT software, thus exploiting the integrated experiment-theory protocol introduced above, is ethanimine (CH_3CHNH), which exists in two isomeric forms (see Figure 5). Ethanamine is a potential prebiotic molecule because it has been postulated to be a possible precursor of amino acids (see, e.g., refs. 159–162). Both isomers of ethanimine have been identified in Sagittarius B2 North, SgrB2(N), using the GBT¹⁶¹. However, the previous experimental works on the rotational spectrum of both isomers were limited to low frequencies, i.e. below 140 GHz.^{161,163,164} As already explained, extrapolations from low-frequency laboratory measurements usually provide inaccurate predictions for higher frequencies; therefore, in view of the extended astronomical observatory facilities provided by ALMA, the extension of the investigation of the rotational spectra for both isomers of ethanimine is warranted. To accomplish this task, an accurate computational study has been performed as detailed in the Methodology section. Quantum-chemical calculations have been carried out using the computational module of VMS-ROT. To improve the prediction of the rotational spectrum, the computed rotational constants were replaced by those available in the literature.¹⁶⁴ The resulting simulated spectra for the two isomers, at $T = 30$ K, are shown in Figure 6, which also highlights the frequency region covered by previous experimental works. From Figure 6 it is evident that, even at such a low temperature, the maximum of intensity is around 200 GHz. The predicted rotational transitions have been subsequently used to guide the experimental investigation of the rotational spectrum.

Table 1 Computed and experimental rotational parameters (values in MHz) of ethanimine.

	<i>E</i> -ethanimine		<i>Z</i> -ethanimine	
	Theory ^a	Experiment ^b	Theory ^a	Experiment ^b
A_0	53178.26	53120.561(30)	50002.63	49964.87(93)
B_0	9780.14	9782.7720(47)	9831.98	9832.4823(96)
C_0	8702.82	8697.0263(46)	8652.81	8646.0305(94)
$\Delta_J \times 10^3$	6.48	6.4641(49)	6.99	6.938(13)
Δ_K	0.568	0.5763(34)	0.468	0.468 ^c
Δ_{JK}	-0.0165	-0.01403(21)	-0.0163	-0.01219(23)
$\delta_J \times 10^3$	1.09	1.1033(19)	1.25	1.2657(65)
δ_K	-0.0535	-0.06709(59)	-0.0522	-0.0642(19)
χ_{aa}	1.03	0.62(11)	-3.62	-3.688(13)
χ_{ab}	-0.46	-0.46 ^c	1.75	1.75 ^c
χ_{bb}	-4.05	-3.78(12)	0.57	0.548(39)
χ_{cc}	3.02	3.16(12)	3.05	3.140(39)
V_3 ^d	563.1	566.37(20)	523.3	517.41(33)
ΔE ^e	0	–	231.5	–

^a Equilibrium CCSD(T)/CBS+CV rotational constants and energies augmented by vibrational corrections at the B2PLYP-D3BJ/maug-cc-pVTZ-dH level. Quartic centrifugal distortion constants at the CCSD(T)/cc-pCVQZ level. Nuclear quadrupole coupling constants at the CCSD(T)/cc-pCVQZ level augmented by vibrational corrections at the B2PLYP-D3(BJ)/maug-cc-pVTZ-dH level. For details, see ref. 17.

^b Watson A-reduction. Values in parenthesis denote one standard deviation and apply to the last digits of the constants.

^c Fixed at the theoretical value.

^d V_3 values in cm^{-1} .

^e Relative energies in cm^{-1} .

Ethanamine has been produced by pyrolysis of a commercial sample of isopropylamine ($(\text{CH}_3)_2\text{CHNH}_2$) and its rotational tran-

sitions have been recorded around 92 GHz (to optimize the experimental conditions) and in the 250–302 GHz frequency range, with an estimated accuracy of 40–60 kHz, by means of the millimeter/submillimeter-wave frequency-modulation spectrometer at the “rotational and computational lab” in Bologna. The presence of a finite V_3 barrier, due to the hindered internal rotation of the methyl group, leads to a splitting of the threefold degeneracy into two levels, a nondegenerate A level and a doubly-degenerate E level, which makes the rotational spectrum rather complicated. The effect of the internal rotation was accurately predicted relying on the quantum-chemical computation of the methyl internal rotation barrier V_3 . The recorded spectra have been analyzed and assigned using the VMS-ROT software, which is able to efficiently treat the A/E splittings observed in the rotational spectra. For the final analysis, all previous measurements have also been incorporated in the fitting procedure. A selection of the spectroscopic parameters is collected in Table 1, which furthermore points out the accuracy of our initial computed data. The reader is referred to ref. 17 for a detailed account on this study.

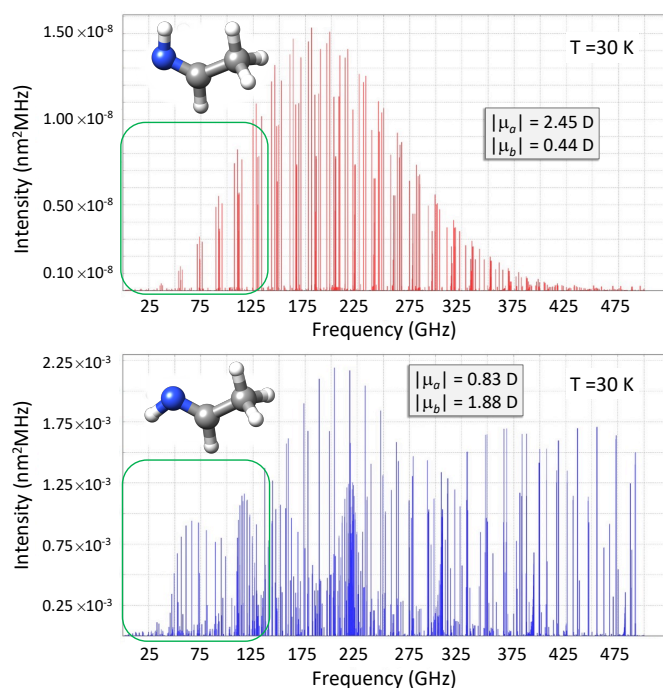


Fig. 6 Simulation of the rotational spectra of *Z*- (top panel) and *E*- CH_3CHNH (bottom panel) at $T = 30$ K obtained with VMS-ROT. The absolute values of the dipole moment components are also reported.

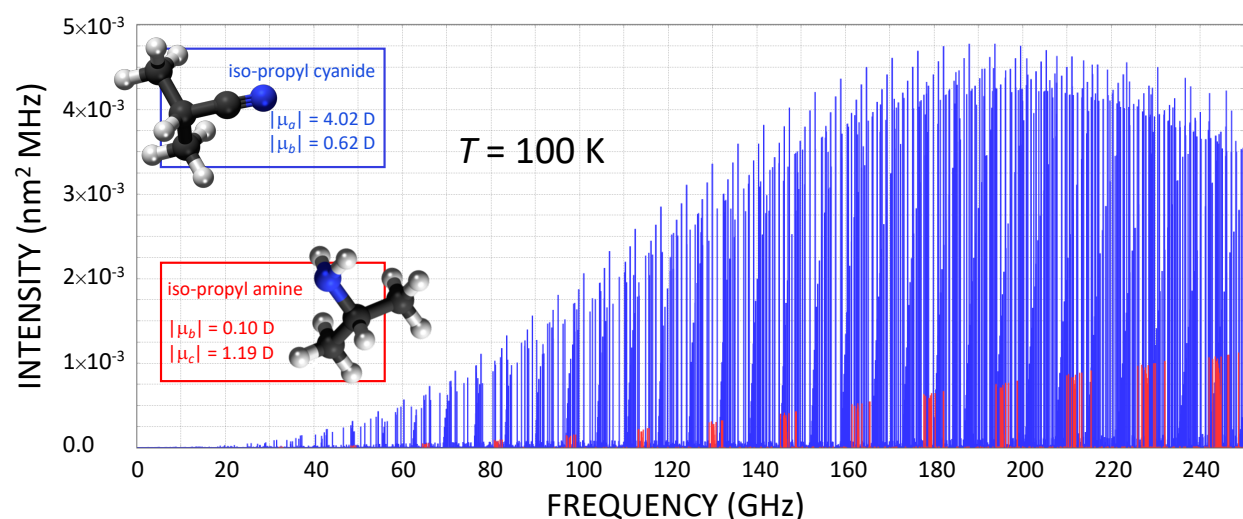


Fig. 7 Simulated rotational spectra of i-propyl amine plotted in red (data from ref. 165) and i-propyl cyanide in blue (data from the Cologne database^{68,69}) at $T = 100$ K.

3.2 Alkyl molecules: amines vs cyanides

Table 2 Rotational constants (in MHz) and dipole moment components (in D) of the most stable conformers of n-/i-propyl cyanide and amine.

<i>anti</i> n-propyl		
	cyanide ^a	amine ^b
A_0	23668.3193(14)	24633.518(12)
B_0	2268.14689(15)	3687.54437(15)
C_0	2152.96395(17)	3473.87413(14)
$ \mu_a $	3.597(59)	0.98
$ \mu_b $	0.984(15)	1.05
$ \mu_c $	0.0	0.0
<i>iso</i> -propyl		
	cyanide ^c	amine ^d
A_0	7940.877174(31)	8331.90303(16)
B_0	3968.087775(27)	7977.33553(17)
C_0	2901.053223(22)	4656.91658(63)
$ \mu_a $	4.0219(50)	0.0
$ \mu_b $	0.0	0.10(4)
$ \mu_c $	0.619(27)	1.19(3)

^a Rotational constants from ref. 166; dipole moment components from ref. 167.

^b *T_t* conformer. Data from ref. 165.

^c Data from ref. 168.

^d *T* conformer. Rotational constants from ref. 165; dipole moment components from ref. 169.

Molecular systems containing the –CN– moiety are considered important prebiotic iCOMs because they can play a role as intermediates in the formation of biologically relevant molecules, such as amino acids. Among these species, different categories can be identified: imines, for which an example has been discussed in the previous section, amines and cyanides. The latter compounds are

widespread in the ISM: from the CN (cyanide) radical and HCN, which are ubiquitous in space, to n-/i-propylcyanide, which are among the largest noncyclic detected molecules^{14,170}. Different is the situation for alkyl amines, with methylamine being the only one identified in the ISM (see, ref. 171 and references therein). While the rotational spectrum of ethylamine is well characterized (in particular, that of the *anti* conformer^{172,173}), limited were the information on the conformers of propylamine prior to a recent study¹⁶⁵. In ref. 165, starting from the two possible structural isomers, namely i-propylamine and n-propylamine, two and five stable conformers –respectively– have been computationally characterized and their rotational spectra investigated by means of an integrated strategy combining high-level quantum-chemical calculations and high-resolution rotational spectroscopy. While the reader is referred to ref. 165 for a detailed account, here, we briefly mention that the “cheap” composite approach was successfully employed for accurately predicting the equilibrium structure (and thus equilibrium rotational constants) and energetics of all conformers. “Cheap” equilibrium rotational constants augmented by B3LYP-D3(BJ)/SNSD¹⁷⁴ vibrational corrections led to the prediction of vibrational ground-state rotational constants with discrepancies of the order of 0.1%. These, combined with quartic and sextic centrifugal distortion constants at the B2PLYP-D3(BJ) and B3LYP-D3(BJ) levels, respectively, provided accurate predictions of the rotational spectra, which made the spectral assignments rather straightforward.

To inspect the possibility of detecting propylamine in space, the rotational constants together with the dipole moment components of the most stable conformers of n-/i-propyl amine and cyanide are compared in Table 2. While n-propyl cyanide exists only in the *anti* and *gauche* forms, with the former being the lowest in energy, for n-propyl amine the number of conformers increases because of different orientations of the –NH₂ group with respect to the alkyl chain, thus leading to five possible conform-

ers, namely Tt , Tg , Gg , Gg' , and Gt^\ddagger . Among them, the most stable is the Tt conformer. As far as the branched isomer is concerned, i-propyl cyanide exists in only one form, whereas i-propyl amine has two conformers, *trans* and *gauche*, with the former being the most stable. From the inspection of Table 2, we note that for both the linear and branched structures, cyanides show larger dipole moment components. This has a strong impact on the intensity of the rotational spectrum, as made it evident in Figure 7 for the i-propyl species. This figure depicts the rotational spectra of i-propyl cyanide (in blue) and of the *trans* conformer of i-propyl amine (in red), simulated at a temperature of 100 K. The actual spectrum of the amine is even weaker than what reported because the simulation of Figure 7 does not take into account that the intensity is also affected by the spreading of the population between two conformers. Using the energy difference from ref. 165, i.e. 2.0 kJ mol^{-1} , at $T = 100 \text{ K}$ the population of the *trans* conformer of i-propyl amine is 56%; therefore, the intensity of the rotational spectrum in Figure 7 should be further reduced by nearly a factor of 2.

The overall conclusion is that, despite the fact that the rotational spectra of the various isomers/conformers of propyl amine have been characterized up to 400 GHz, the chances of detecting any rotational features in radioastronomical line surveys are poor; however, they might be hidden in their confusion limit and, indeed, increase it.

3.3 A key prebiotic molecule: cyanomethanimine

As already mentioned, the iCOMs containing the cyano group are important prebiotic molecules. In this context, an interesting species is cyanomethanimine, which exists in three different structural and conformational isomers: N-cyanomethanimine and C-cyanomethanimine, the latter existing in the *E* and *Z* forms (see Figure 8). In the following, we will focus on C-cyanomethanimine (HNCHCN), simply denoted as cyanomethanimine, for which both isomers have been recently detected^{13,18}.

The identification of *E*-cyanomethanimine in Sgr B2(N) in the GBT PRIMOS survey by Zaleski et al.¹³ has prompted two different studies: the quantum-chemical investigation of a feasible gas-phase formation route³⁷ and the extension of laboratory measurements of the rotational spectra for both isomers at frequencies higher than 100 GHz²³. The spectroscopic study was spurred by the fact that the rotational spectra of both *E* and *Z* forms show a maximum of intensity at frequencies higher than 100 GHz already at $T = 10 \text{ K}$ for *E*-cyanomethanimine and at $T = 30 \text{ K}$ for the *Z* isomer. For these reasons, in ref. 23, the rotational spectrum of cyanomethanimine has been investigated in the 100-117 GHz and 240-419 GHz frequency regions by means of the millimeter/submillimeter-wave frequency modulated spectrometer at the “rotational and computational lab” in Bologna,

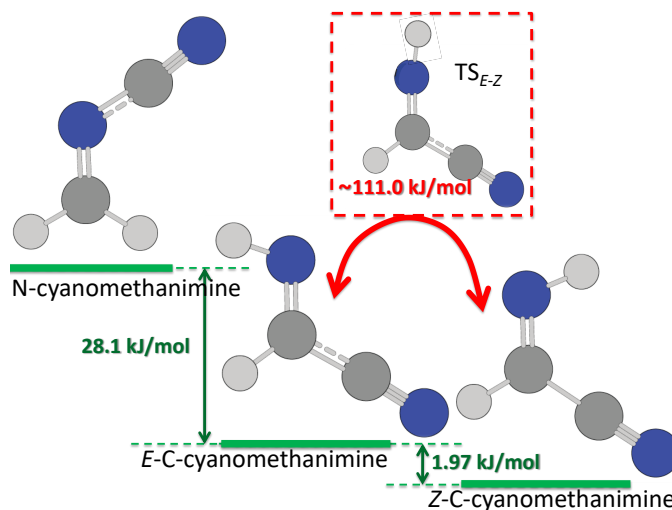


Fig. 8 Isomers of cyanomethanimine. ZPE-corrected relative energies are reported: for minima, relative electronic energies at the CCSD(T)/CBS+CV+fT+fQ level are augmented by anharmonic ZPE corrections (harmonic part at the all-CCSD(T)/cc-pCVQZ level, anharmonic terms at the fc-CCSD(T)/cc-pVTZ level); for the TS_{E-Z} , the relative electronic energy at the CCSD(T)/CBS+CV level is corrected for harmonic ZPE at the fc-CCSD(T)/cc-pVTZ level. Values taken from ref. 175.

thus providing accurate predictions of the rotational signatures up to $\sim 700 \text{ GHz}$. Using them, a search for cyanomethanimine emissions toward nearby Sun-like-star forming regions has been performed using the ASAI IRAM 30-m dataset[§], thereby investigating the earliest stages of the star forming process, from starless regions to the more evolved hot-corinos associated with both Class 0 and Class I objects. While such astronomical searches did not lead to any line identification, the study of ref. 23 allowed the derivation of upper limits of 10^{11} - 10^{12} cm^{-2} for the cyanomethanimine column density.

In ref. 37, a gas-phase formation pathway, based on the reaction between the CN radical and methanimine (CH_2NH), both widely diffuse species, was investigated under the characteristic conditions of the ISM, and it was demonstrated to efficiently produce cyanomethanimine. Furthermore, the formation of the most stable *Z*-cyanomethanimine was found to be favored by a factor of ~ 1.5 with respect to the *E* form, which –however– cannot explain the relative abundance ratio between the *Z* and *E* isomers ($[Z]/[E]$) of about 6 derived in ref. 18. While this discrepancy is under investigation in our laboratories, the focus is here on the crucial importance of accurate quantum-chemical calculations.

The CBS-QB3 composite approach was employed in ref. 37 for the energetic characterization of the reactive PES. As already pointed in ref. 175, this level of theory showed some limitations in correctly describing the *Z*-/*E*-cyanomethanimine isomerization, probably because of the use of B3LYP/6-31G(d) geometry optimizations and ZPEs as well as the empirical corrections introduced in the model. To improve the energetic description of the

[‡] The capital letter refers to the conformation of the NCCC dihedral angle, with *T* standing for *trans* and *G* for *gauche*. The lower-case letter refers to the value of the :NCC dihedral angle, with “.” denoting the nitrogen lone pair. For the latter dihedral angle, starting from the *trans* (*t*) position, clockwise and counterclockwise rotations of the NH_2 group by 120 degrees along the NC bond lead to *g* and *g'*, respectively.

[§] <http://www.oan.es/asai/>

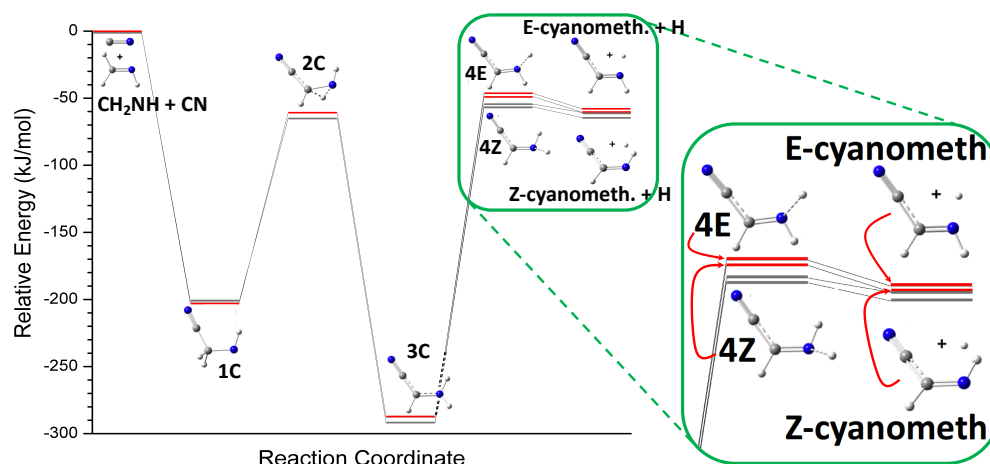
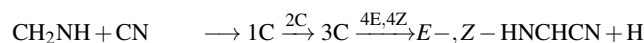
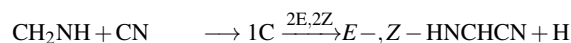


Fig. 9 $\text{CH}_2\text{NH} + \text{CN} \rightarrow \text{Z-/E-cyanomethanimine}$: path 1. Comparison of the relative electronic energies: CBS-QB3 results from ref. 37 in grey, CBS+CV+ft+pQ results (this work) in red.

two paths accessible at low temperatures identified in ref. 37:



(Path 1 : Figure 9)



(Path 2 : Figure 10)

the stationary points have been optimized at the B2PLYP-D3(BJ)/jun-cc-pVTZ¹²⁹ level and single-point energy calculations have been performed using the composite scheme of eq. (7), with the contribution of quadruple excitations taken into account using the CCSDT(Q) model. In addition, the performance of the “cheap” approach (see Eq. (8)) has been checked. In both cases, for open-shell species, MP2 and CCSD(T) calculations have been carried out by using the ROHF reference wavefunction. The results are collected in Table 3.

From the inspection of Table 3, and Figures 9 and 10, it is evident that all reaction barriers computed at the CBS-QB3 level are underestimated by about 4 to 10 kJ mol^{-1} , while confirming that the path 1 is favored with respect to path 2. On the contrary, despite its limited computational cost, the “cheap” scheme performs better: it provides results improved with respect to CBS-QB3 and similar in accuracy (if not better) to those issued from the CCSD(T)/CBS+CV model. While the investigation of the rate constant is outside the scope of the present study, our results suggest that the reaction is slower than what determined in ref. 37.

In Table 3, the energetic values at the fc-CCSD(T)/cc-pVTZ level are also reported for comparison purposes. In fact, this level of theory is often employed in theoretical investigations of reaction mechanisms for astrochemical purposes. However, it does not fulfil the so-called chemical accuracy, with reaction barriers that can even deviate by more than 10 kJ mol^{-1} from the CCSD(T)/CBS+CV+DBOC+rel+ft+pQ values. In this respect, it is worthwhile noting that the fc-CCSD(T)/cc-pVTZ level of theory is the cost-determining step of the “cheap” approach and, with a very limited additional computational cost, the accuracy can be

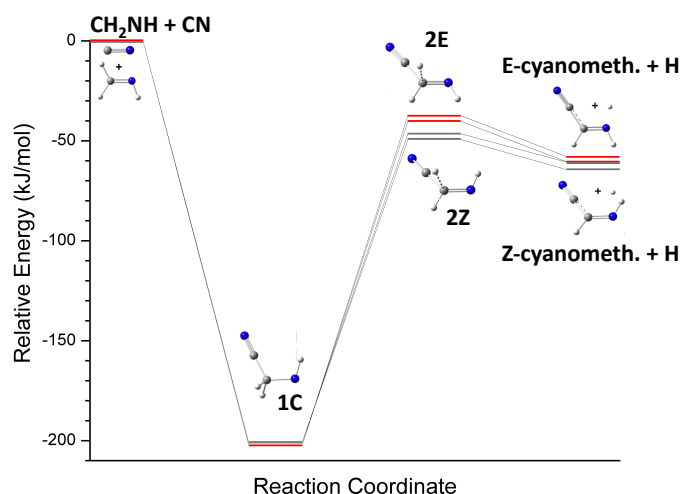


Fig. 10 $\text{CH}_2\text{NH} + \text{CN} \rightarrow \text{Z-/E-cyanomethanimine}$: path 2. Comparison of the relative electronic energies: CBS-QB3 results from ref. 37 in grey, CBS+CV+ft+pQ results (this work) in red.

significantly improved.

The last point that deserves to be addressed concerns the use of the ZPE-corrected energy difference between the two cyanomethanimine isomers (ΔE_0) to derive the kinetic temperature (T_K) of the G+0.693 cloud (where both isomers have been recently detected¹⁸). Using the abundance $[\text{Z}]/[\text{E}]$ ratio obtained in ref. 18, i.e. 6.2, and the ΔE_0 of 1.97 kJ mol^{-1} (237.5 K) from ref. 175, employing the expression:

$$[\text{Z}]/[\text{E}] = \frac{1}{g} \times \frac{\Delta E_0}{T_K}, \quad (9)$$

a value of 130.2 K is obtained for the kinetic temperature (g , which accounts for statistical weight, being = 1 in this case) that well agrees with the 73-140 K range derived in ref. 176, thus suggesting that in G+0.693 the two isomers are in, or close to, thermodynamic equilibrium.

Table 3 Relative energies (kJ mol⁻¹) for the methanime + CN → Z-/E-C-cyanomethanimine reaction.^a

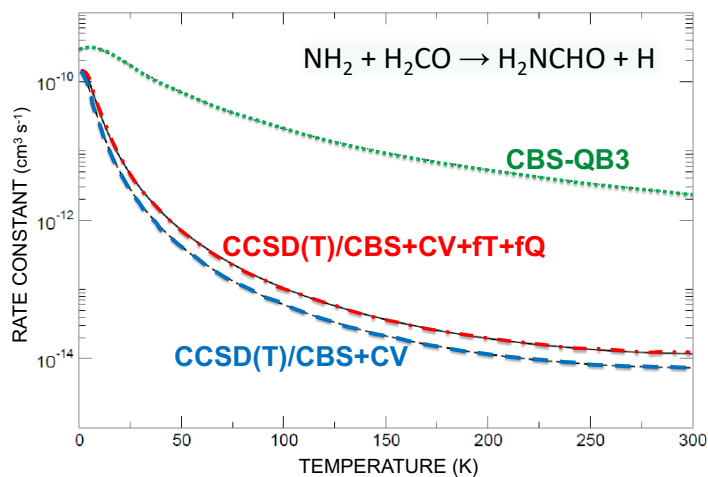
	fc-CCSD(T)/ cc-pVTZ	CBS+CV ^b	CBS+CV ^c +DBOC+rel	CBS+CV ^d +DBOC+rel +fT+pQ	cheap ^e	CBS-QB3 ^f
Precursors (CH ₂ NH+CN)	0.0	0.0	0.0	0.0	0.0	0.0
1C	-200.07	-206.52	-206.27	-202.56	-203.59	-201.3
2C (TS)	-55.47 (144.60)	-65.18 (141.34)	-64.20 (142.07)	-60.66 (141.90)	-63.55 (140.04)	-64.9 (136.4)
2E (TS)	-32.69 (167.38)	-40.39 (166.13)	-40.17 (166.10)	-37.37 (165.18)	-37.97 (165.62)	-46.4 (154.8)
2Z (TS)	-35.96 (164.11)	-43.1646 (163.36)	-42.96 (163.30)	-40.23 (162.32)	-40.62 (162.97)	-49.4 (151.9)
3C	-271.24	-287.92	-287.37	-287.93	-284.59	-292.0
4E (TS)	-42.06 (229.18)	-49.31 (238.61)	-49.12 (238.25)	-46.48 (241.45)	-46.22 (238.37)	-54.4 (237.6)
4Z (TS)	-44.80 (226.44)	-51.51 (236.41)	-51.35 (236.02)	-48.82 (239.11)	-48.37 (235.89)	-56.5 (235.5)
E-HNCHCN+H	-56.04	-60.88	-61.42	-57.91	-58.55	-60.7
Z-HNCHCN+H	-59.05	-63.30	-63.87	-60.44	-60.89	-64.4

^a Barriers with respect to the preceding intermediate are given within parentheses.^b CCSD(T)/CBS+CV energies. See text.^c CCSD(T)/CBS+CV energies augmented by DBOC and relativistic contributions. See text.^d CCSD(T)/CBS+CV+DBOC+rel augmented by fT and pQ contributions. See text.^e "cheap" composite scheme. See text.^f From ref. 37.

3.4 Gas-phase formation of formamide in the ISM

Formamide (H₂NCHO) is an ubiquitous molecule that has been detected in many sources throughout the universe¹⁷⁷. Among iCOMS, formamide is thought to play a central role because it can polymerize through biocatalyzed processes to provide all five nucleobases of DNA and RNA as well as carboxylic and amino acids^{178,179}. Therefore, formamide is the compound that can connect metabolism (conversion of energy), ruled by proteins, and genetics (passage of information), ruled by DNA and RNA¹⁷⁸. Despite its wide distribution in the universe, the mechanism by which formamide is formed is still a subject of intense debate¹⁸⁰: both gas-phase (see, e.g., refs. 33,181) and grain surface mechanisms (see, e.g., refs. 46,182) have been proposed.

In the present context, the gas-phase formation route of formamide has been chosen because it provides a remarkable example in order to point out the need of highly accurate quantum-chemical calculations when investigating pathways that should be feasible at very low temperatures as well as to demonstrate that astronomical observations can be used to support the conclusions drawn by theoretical studies. To address the first point, we refer to the works carried out in refs. 33,183, which both considered the NH₂ + H₂CO → H₂NCHO + H reaction. While the CBS-QB3 approach was employed in ref. 183, in the subsequent investigation³³, the level of theory was improved by exploiting the CCSD(T)/CBS+CV and CCSD(T)/CBS+CV+fT+fQ composite schemes. As already noted for the formation pathway of cyanomethanimine, the CBS-QB3 level underestimates the reaction barriers. This strongly affects the reaction rate, as well

**Fig. 11** Rate constant (logarithmic scale) as a function of temperature for the NH₂ + H₂CO → H₂NCHO + H reaction. CCSD(T)/CBS+CV and CCSD(T)/CBS+CV+fT+fQ results from ref. 33, CBS-QB3 results from ref. 183.

evidenced by Figure 11, with the rate constant decreasing by two orders of magnitude.

The critical role played by the accuracy of electronic energy calculations is also pointed out by Figure 12 (for more details on the reaction mechanisms and labelling of intermediates, the reader is referred to ref. 33), the effect of the level of theory being addressed for the transition state. Since TS6 is slightly submerged, but it emerges above the precursors once anharmonic

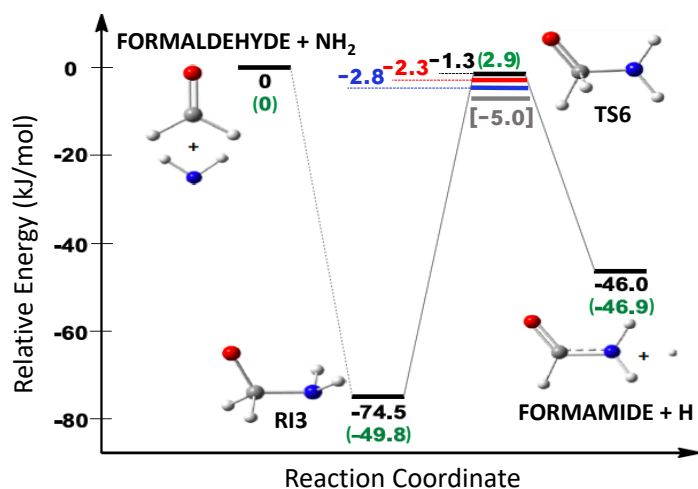


Fig. 12 Mechanism for the $\text{NH}_2 + \text{H}_2\text{CO} \rightarrow \text{H}_2\text{NCHO} + \text{H}$ reaction: relative energies at the CCSD(T)/CBS+CV level in black, CCSD(T)/CBS+CV+fT in red and CCSD(T)/CBS+CV+fT+fQ in blue; the CCSD(T)/CBS+CV results augmented by anharmonic ZPEs (B2PLYP-D3/m-aug-cc-pVTZ) are in green within parentheses. Data taken from ref. 33. For TS6, the CBS-QB3 relative energy (in grey)¹⁸³ is also provided.

ZPE corrections are incorporated, its relative energy has an impact on the overall rate constant. As already mentioned, at the low temperatures characteristic of the ISM, rates are exquisitely sensitive to energetics and kinetic barrier heights. Therefore, the relative energy of TS6 decreasing from a value of -1.3 kJ mol^{-1} at the CCSD(T)/CBS+CV level to -2.8 kJ mol^{-1} when employing the CCSD(T)/CBS+CV+fT+fQ approach leads to an increase of the rate constant of about 30%, from $7.6 \times 10^{-11} \text{ cm}^3 \text{ s}^{-1}$ to $9.9 \times 10^{-11} \text{ cm}^3 \text{ s}^{-1}$, at $T = 5 \text{ K}$.

Recent astronomical observations of the formamide rotational line lying at 81.7 GHz ($J = 4_{1,4} - 3_{1,3}$), obtained in the framework of the large program SOLIS (Seeds Of Life In Space) at IRAM NOEMA (Northern Extended Millimeter Array)⁴⁴, have supported the reliability of the formation route proposed in ref. 33. Indeed, the work of ref. 44 was able to demonstrate that formamide detected in L1157-B1 should have been produced by gas-phase chemistry, with the $\text{NH}_2 + \text{H}_2\text{CO} \rightarrow \text{H}_2\text{NCHO} + \text{H}$ reaction being able to explain the astronomical observations. In conclusion, ref. 44 provided an additional evidence that gas-phase chemistry plays an important role in the formation of iCOMs, thus further challenging pure grain-surface chemistry paradigms, already questioned by recent detections of iCOMs in cold objects (see, e.g., ref. 184).

4 Concluding remarks

Unthinkable a half-century ago, the discovery of molecules in space showing a certain degree of complexity, and in particular those with a prebiotic character, is proceeding at a nearly constant rate¹¹. Debate on their origins has been further stimulated by the identification of biomolecule building blocks, such as nucleobases and amino acids, in meteorites and comets. Since many of the molecules found in space play a role in the chemistry of

life, the question of their molecular genesis and evolution might be related to the profound question of the origin of life itself. Understanding the underlying chemical processes, including the production, reactions and destruction of compounds, requires the concomitant study of gas-phase reactivity and heterogeneous processes on dust-grains.

Despite increasing efforts, we are far from resolving most of the above challenges, and –in particular– far from having a complete census of interstellar molecules and a clear understanding on how they are formed. On these grounds, this perspective was meant to provide an overview on strategies that are currently pursued in order to gain new insights with respect to both issues. It has been shown how a fruitful interplay of experiment and theory in the field of rotational spectroscopy allows for obtaining accurate rest frequencies to be used for astronomical searches. Moving to formation pathways, quantum chemistry is nowadays able to provide a quantitative picture of the reaction mechanisms occurring in the gas phase under the extreme conditions of the ISM, provided that the level of theory is suitably chosen.

To go a step forward, in our opinion, the complex scenario of astrochemistry requires a cutting-edge, powerful approach that integrates experimental and theoretical studies and advances with large-scale numerical simulations and Big Data analysis, further strengthened by immersive virtual and augmented reality environments, thus enabling a natural interaction with phenomena spanning several space and time scales^{116,185}. To make the computational part of the platform as general as possible, several theoretical/computational developments need to be introduced. At the same time, local computational resources for development and test need be coupled with “in the cloud” resources for production and large-scale calculations. Existing laboratories for experimental molecular spectroscopy need also to be fully integrated, thereby relying on newly developed augmented- and virtual-reality tools. Work along these lines –already started in our and other laboratories– will surely enable a number of applications well beyond the state of the art in the field of astrochemistry and will pave the route toward the investigation of a further degree of chemical complexity in space: from the prebiotic building blocks to biomolecules^{178,186–188}.

Conflicts of interest

“There are no conflicts to declare”.

Acknowledgements

This work has been supported by MIUR “PRIN 2015” funds (Grant Number 2015F59J3R) and by the University of Bologna (RFO funds). Authors gratefully thank Dr. Spada for his help with some figures.

Notes and references

- 1 J. Hartmann, *Astrophys. J.*, 1904, **19**, 268–286.
- 2 R. J. Trumpler, *Publ. Astronom. Soc. Pac.*, 1930, **42**, 214.
- 3 E. Herbst and E. F. van Dishoeck, *Ann. Rev. Astron. Astrophys.*, 2009, **47**, 427–480.
- 4 J. M. Hollis, F. J. Lovas and P. R. Jewell, *Astrophys. J.*, 2000, **540**, L107–L110.

- 5 J. M. Hollis, F. J. Lovas, A. J. Remijan, P. R. Jewell, V. V. Ilyushin and I. Kleiner, *Astrophys. J.*, 2006, **643**, L25–L28.
- 6 Belloche, A., Menten, K. M., Comito, C., Müller, H. S. P., Schilke, P., Ott, J., Thorwirth, S. and Hieret, C., *Astron. Astrophys.*, 2008, **482**, 179–196.
- 7 Belloche, A., Menten, K. M., Comito, C., Müller, H. S. P., Schilke, P., Ott, J., Thorwirth, S. and Hieret, C., *Astron. Astrophys.*, 2008, **492**, 769–773.
- 8 B. A. McGuire, P. B. Carroll, R. A. Loomis, I. A. Finneran, P. R. Jewell, A. J. Remijan and G. A. Blake, *Science*, 2016, **352**, 1449–1452.
- 9 S. Yamamoto, *Introduction to Astrochemistry (Chemical Evolution from Interstellar Clouds to Star and Planet Formation)*, Springer, 2017.
- 10 A. G. G. M. Tielens, *Rev. Mod. Phys.*, 2013, **85**, 1021–1081.
- 11 B. A. McGuire, *Astrophys. J. Suppl. Ser.*, 2018, **239**, 17.
- 12 J. Tennyson, *Astronomical Spectroscopy*, Imperial College Press, 2005.
- 13 D. P. Zaleski, N. A. Seifert, A. L. Steber, M. T. Muckle, R. A. Loomis, J. F. Corby, O. Martinez, K. N. Crabtree, P. R. Jewell, J. M. Hollis, F. J. Lovas, D. Vasquez, J. Nyiramahirwe, N. Sciortino, K. Johnson, M. C. McCarthy, A. J. Remijan and B. H. Pate, *Astrophys. J.*, 2013, **765**, L10.
- 14 A. Belloche, R. T. Garrod, H. S. P. Müller and K. M. Menten, *Science*, 2014, **345**, 1584–1587.
- 15 A. Coutens, J. K. Jørgensen, M. H. D. van der Wiel, H. S. P. Müller, J. M. Lykke, P. Bjerkeli, T. L. Bourke, H. Calcutt, M. N. Drozdovskaya, C. Favre, E. C. Fayolle, R. T. Garrod, S. K. Jacobsen, N. F. W. Ligterink, K. I. Öberg, M. V. Persson, E. F. van Dishoeck and S. F. Wampfler, *Astron. Astrophys.*, 2016, **590**, L6.
- 16 S. Spezzano, H. Gupta, S. Brünken, C. A. Gottlieb, P. Caselli, K. M. Menten, H. S. P. Müller, L. Bizzocchi, P. Schilke, M. C. McCarthy and S. Schlemmer, *Astron. Astrophys.*, 2016, **586**, A110.
- 17 A. Melli, M. Melosso, N. Tasinato, G. Bosi, L. Spada, J. Bloino, M. Mendolicchio, L. Dore, V. Barone and C. Puzzarini, *Astrophys. J.*, 2018, **855**, 123.
- 18 V. M. Rivilla, J. Martin-Pintado, I. Jimenez-Serra, S. Zeng, S. Martin, J. Armijos-Abendano, M. A. Requena-Torres, R. Aladro and D. Riquelme, *Mon. Not. R. Astron. Soc.*, 2019, **483**, L114–L119.
- 19 A. Belloche, R. T. Garrod, H. S. P. Müller, K. M. Menten, I. Medvedev, J. Thomas and Z. Kisiel, *Astron. Astrophys.*, 2019, **628**, A10.
- 20 T. J. Balle and W. H. Flygare, *Rev. Sci. Instrum.*, 1981, **52**, 33.
- 21 J.-U. Grabow, W. Stahl and H. Dreizler, *Rev. Sci. Instrum.*, 1996, **67**, 4072.
- 22 F. C. De Lucia, *J. Mol. Spectrosc.*, 2010, **261**, 1–17.
- 23 M. Melosso, A. Melli, C. Puzzarini, C. Codella, L. Spada, L. Dore, C. D. Esposti, B. Lefloch, R. Bachiller, C. Ceccarelli, J. Cernicharo and V. Barone, *Astron. Astrophys.*, 2018, **609**, A121.
- 24 H. F. Schaefer, *Science*, 1986, **231**, 1100–1107.
- 25 W. D. Allen, A. L. L. East and A. G. Császár, *Structures and Conformations of Non-Rigid Molecules*, Kluwer, Dordrecht, 1993, pp. 343–373.
- 26 C. Puzzarini, J. F. Stanton and J. Gauss, *Int. Rev. Phys. Chem.*, 2010, **29**, 273–367.
- 27 *Computational Spectroscopy: Methods, Experiments and Applications*, ed. J. Grunenberg, John Wiley & Sons, Inc., 2010.
- 28 K. A. Peterson, D. Feller and D. Dixon, *Theor. Chem. Acc.*, 2012, **113**, 1079/1–20.
- 29 C. Puzzarini, *Phys. Chem. Chem. Phys.*, 2013, **15**, 6595–6607.
- 30 V. Barone, M. Biczysko and C. Puzzarini, *Acc. Chem. Res.*, 2015, **48**, 1413–1422.
- 31 M. Biczysko, J. Bloino and C. Puzzarini, *WIREs Comput. Mol. Sci.*, 2018, **8**, e1349.
- 32 C. Puzzarini, J. Bloino, N. Tasinato and V. Barone, *Chem. Rev.*, 2019, **119**, 8131–8191.
- 33 F. Vazart, D. Calderini, C. Puzzarini, D. Skouteris and V. Barone, *J. Chem. Theory Comput.*, 2016, **12**, 5385–5397.
- 34 I. W. M. Smith, D. Talbi and E. Herbst, *Astron. Astrophys.*, 2001, **369**, 611–615.
- 35 S. Rampino, M. Pastore, E. Garcia, L. Pacifici and A. Laganá, *Mon. Not. R. Astron. Soc.*, 2016, **460**, 2368–2375.
- 36 D. Skouteris, N. Balucani, N. Faginas-Lago, S. Falcinelli and M. Rosi, *Astron. Astrophys.*, 2015, **584**, A76.
- 37 F. Vazart, C. Latouche, D. Skouteris, N. Balucani and V. Barone, *Astrophys. J.*, 2015, **810**, 111.
- 38 J. Enrique-Romero, A. Rimola, C. Ceccarelli and N. Balucani, *Mon. Not. R. Astron. Soc.*, 2016, **459**, L6–L10.
- 39 J. A. Miller and S. J. Klippenstein, *J. Phys. Chem. A*, 2006, **110**, 10528–10544.
- 40 D. Skouteris, F. Vazart, C. Ceccarelli, N. Balucani, C. Puzzarini and V. Barone, *Mon. Not. R. Astron. Soc. Lett.*, 2017, **468**, L1.
- 41 T. L. Nguyen, J. F. Stanton and J. R. Barker, *Chem. Phys. Lett.*, 2010, **499**, 9–15.
- 42 A. Fernández-Ramos, J. A. Miller, S. J. Klippenstein and D. G. Truhlar, *Chem. Rev.*, 2006, **106**, 4518–4584.
- 43 A. Zanchet, F. Lique, O. Roncero, J. R. Goicoechea and N. Bulut, *Astron. Astrophys.*, 2019, **626**, A103.
- 44 C. Codella, C. Ceccarelli, P. Caselli, N. Balucani, V. Barone, F. Fontani, B. Lefloch, L. Podio, S. Viti, S. Feng, R. Bachiller, E. Bianchi, F. Dulieu, I. Jiménez-Serra, J. Holdship, R. Neri, J. E. Pineda, A. Pon, I. Sims, S. Spezzano, A. I. Vasyunin, F. Alves, L. Bizzocchi, S. Bottinelli, E. Caux, A. Chacón-Tanarro, R. Choudhury, A. Coutens, C. Favre, P. Hily-Blant, C. Kahane, A. Jaber Al-Edhari, J. Laas, A. López-Sepulcre, J. Ospina, Y. Oya, A. Punanova, C. Puzzarini, D. Quenard, A. Rimola, N. Sakai, D. Skouteris, V. Taquet, L. Testi, P. Theulé, P. Ugliengo, C. Vastel, F. Vazart, L. Wiesenfeld and S. Yamamoto, *Astron. Astrophys.*, 2017, **605**, L3.
- 45 A. Horn, H. Møllendal, O. Sekiguchi, E. Uggerud, H. Roberts, E. Herbst, A. A. Viggiano and T. D. Fridgen, *Astrophys. J.*,

- 2004, 611, 605–614.
- 46 R. T. Garrod, S. L. W. Weaver and E. Herbst, *Astrophys. J.*, 2008, 682, 283–302.
 - 47 E. Herbst, *Phys. Chem. Chem. Phys.*, 2014, 16, 3344–3359.
 - 48 A. Bacmann, V. Taquet, A. Faure, C. Kahane and C. Ceccarelli, *Astron. Astrophys.*, 2012, 541, L12.
 - 49 R. T. Garrod and S. L. Widicus Weaver, *Chem. Rev.*, 2013, 113, 8939–8960.
 - 50 V. Barone, *WIREs Comput. Mol. Sci.*, 2016, 6, 86–110.
 - 51 D. Licari, A. Baiardi, M. Biczysko, F. Egidi, C. Latouche and V. Barone, *J. Comput. Chem.*, 2015, 36, 321–334.
 - 52 For information and download, see <http://dreamslab.sns.it/vms/>.
 - 53 V. Barone, A. Baiardi, M. Biczysko, J. Bloino, C. Cappelli and F. Lipparini, *Phys. Chem. Chem. Phys.*, 2012, 14, 12404–12422.
 - 54 V. Barone, A. Baiardi and J. Bloino, *Chirality*, 2014, 26, 588–600.
 - 55 J. Bloino, M. Biczysko and V. Barone, *J. Phys. Chem. A*, 2015, 119, 11862–11874.
 - 56 D. Licari, N. Tasinato, L. Spada, C. Puzzarini and V. Barone, *J. Chem. Theory Comput.*, 2017, 13, 4382–4396.
 - 57 M. J. Frisch, G. W. Trucks, H. B. Schlegel, G. E. Scuseria, M. A. Robb, J. R. Cheeseman, G. Scalmani, V. Barone, G. A. Petersson, H. Nakatsuji, X. Li, M. Caricato, A. V. Marenich, J. Bloino, B. G. Janesko, R. Gomperts, B. Mennucci, H. P. Hratchian, J. V. Ortiz, A. F. Izmaylov, J. L. Sonnenberg, D. Williams-Young, F. Ding, F. Lipparini, F. Egidi, J. Goings, B. Peng, A. Petrone, T. Henderson, D. Ranasinghe, V. G. Zakrzewski, J. Gao, N. Rega, G. Zheng, W. Liang, M. Hada, M. Ehara, K. Toyota, R. Fukuda, J. Hasegawa, M. Ishida, T. Nakajima, Y. Honda, O. Kitao, H. Nakai, T. Vreven, K. Throssell, J. A. Montgomery, Jr., J. E. Peralta, F. Ogliaro, M. J. Bearpark, J. J. Heyd, E. N. Brothers, K. N. Kudin, V. N. Staroverov, T. A. Keith, R. Kobayashi, J. Normand, K. Raghavachari, A. P. Rendell, J. C. Burant, S. S. Iyengar, J. Tomasi, M. Cossi, J. M. Millam, M. Klene, C. Adamo, R. Cammi, J. W. Ochterski, R. L. Martin, K. Morokuma, O. Farkas, J. B. Foresman and D. J. Fox, *Gaussian 16 Revision A.03*, 2016, Gaussian Inc. Wallingford CT.
 - 58 J. F. Stanton, J. Gauss, M. E. Harding and P. G. Szalay, *CFOUR. A quantum chemical program package*, 2016, with contributions from A. A. Auer, R. J. Bartlett, U. Benedikt, C. Berger, D. E. Bernholdt, Y. J. Bomble, O. Christiansen, F. Engel, M. Heckert, O. Heun, C. Huber, T.-C. Jagau, D. Jonsson, J. Jusélius, K. Klein, W. J. Lauderdale, F. Lipparini, D. Matthews, T. Metzroth, L. A. Mück, D. P. O'Neill, D. R. Price, E. Prochnow, C. Puzzarini, K. Ruud, F. Schiffmann, W. Schwalbach, S. Stopkowicz, A. Tajti, J. Vázquez, F. Wang, J. D. Watts and the integral packages MOLECULE (J. Almlöf and P. R. Taylor), PROPS (P. R. Taylor), ABACUS (T. Helgaker, H. J. Aa. Jensen, P. Jørgensen, and J. Olsen), and ECP routines by A. V. Mitin and C. van Wüllen. For the current version, see <http://www.cfour.de>.
 - 59 H. M. Pickett, *J. Mol. Spectrosc.*, 1991, 148, 371–377.
 - 60 W. Gordy and R. L. Cook, *Microwave Molecular Spectra*, 3rd Edition, Wiley, New York, 1984.
 - 61 M. R. Aliev and J. K. G. Watson, *Molecular Spectroscopy: Modern Research*, Academic Press, 1985, vol. 3, pp. 1–67.
 - 62 J. K. G. Watson, *J. Chem. Phys.*, 1968, 48, 4517–4524.
 - 63 I. M. Mills, *Molecular Spectroscopy: Modern Research*, Academic Press, New York, 1972, ch. 3.2, pp. 115–140.
 - 64 W. H. Flygare, *Chem. Rev.*, 1974, 74, 653–687.
 - 65 J. Gauss, K. Ruud and T. Helgaker, *J. Chem. Phys.*, 1996, 105, 2804–2812.
 - 66 C. Puzzarini, J. Heckert and J. Gauss, *J. Chem. Phys.*, 2008, 128, 194108.
 - 67 J. K. G. Watson, *Vibrational spectra and structure. A series of advances*, Elsevier, Amsterdam, Netherlands, 1977, vol. 6, pp. 1–89.
 - 68 H. S. P. Müller, S. Thorwirth, D. A. Roth and G. Winnewisser, *Astron. Astrophys.*, 2001, 370, L49–L52.
 - 69 H. S. P. Müller, F. Schlöder, J. Stutzki and G. Winnewisser, *J. Mol. Struct.*, 2005, 742, 215–227.
 - 70 B. A. McGuire, C. L. Brogan, T. R. Hunter, A. J. Remijan, G. A. Blake, A. M. Burkhardt, P. B. Carroll, E. F. van Dishoeck, R. T. Garrod, H. Linnartz, C. N. Shingledecker and E. R. Willis, *Astrophys. J.*, 2018, 863, L35.
 - 71 D. Feller, *J. Chem. Phys.*, 1993, 98, 7059.
 - 72 J. M. Martin and P. R. Taylor, *Chem. Phys. Lett.*, 1996, 248, 336–344.
 - 73 M. Heckert, M. Kállay and J. Gauss, *Mol. Phys.*, 2005, 103, 2109.
 - 74 M. Heckert, M. Kállay, D. P. Tew, W. Klopper and J. Gauss, *J. Chem. Phys.*, 2006, 125, 044108.
 - 75 M. S. Schuurman, W. D. Allen, P. von Ragué Schleyer and H. F. Schaefer III, *J. Chem. Phys.*, 2005, 122, 104302.
 - 76 M. S. Schuurman, S. R. Muir, W. D. Allen and H. F. Schaefer, *J. Chem. Phys.*, 2004, 120, 11586–11599.
 - 77 A. Karton and J. M. L. Martin, *J. Chem. Phys.*, 2012, 136, 124114.
 - 78 W. J. Morgan, D. A. Matthews, M. Ringholm, J. Agarwal, J. Z. Gong, K. Ruud, W. D. Allen, J. F. Stanton and H. F. Schaefer, *J. Chem. Theory Comput.*, 2018, 14, 1333–1350.
 - 79 A. Tajti, P. G. Szalay, A. G. Császár, M. Kállay, J. Gauss, E. F. Valeev, B. A. Flowers, J. Vázquez and J. F. Stanton, *J. Chem. Phys.*, 2004, 121, 11599–11613.
 - 80 A. D. Boese, M. Oren, O. Atasoylu, J. M. L. Martin, M. Kállay and J. Gauss, *J. Chem. Phys.*, 2004, 120, 4129–4141.
 - 81 A. Karton, E. Rabinovich, J. M. L. Martin and B. Ruscic, *J. Chem. Phys.*, 2006, 125, 144108.
 - 82 K. Raghavachari, G. W. Trucks, J. A. Pople and M. Head-Gordon, *Chem. Phys. Lett.*, 1989, 157, 479–483.
 - 83 C. Puzzarini and V. Barone, *Phys. Chem. Chem. Phys.*, 2011, 13, 7189–7197.
 - 84 C. Møller and M. S. Plesset, *Phys. Rev.*, 1934, 46, 618–622.
 - 85 J. Demaison, L. Margulès and J. E. Boggs, *Struct. Chem.*, 2003, 14, 159–174.

- 86 K. A. Peterson and T. H. Dunning, *J. Mol. Struct. THEOCHEM*, 1997, 400, 93–117.
- 87 P. Botschwina, T. Merzliak, B. Schulz and A. Heyl, *J. Mol. Struct.*, 2000, 517–518, 301–306.
- 88 B. Schroder, O. Weser, P. Sebald and P. Botschwina, *Mol. Phys.*, 2015, 113, 1914–1923.
- 89 A. G. Császár, W. D. Allen and H. F. Schaefer III, *J. Chem. Phys.*, 1998, 108, 9751–9764.
- 90 D. P. Tew, W. Klopper, M. Heckert and J. Gauss, *J. Phys. Chem. A*, 2007, 111, 11242–11248.
- 91 V. Barone, M. Biczysko, J. Bloino and C. Puzzarini, *Phys. Chem. Chem. Phys.*, 2013, 15, 10094–10111.
- 92 C. Puzzarini, M. Biczysko and V. Barone, *J. Chem. Theory Comput.*, 2010, 6, 828–838.
- 93 C. Puzzarini, M. Biczysko and V. Barone, *J. Chem. Theory Comput.*, 2011, 7, 3702–3710.
- 94 S. Alessandrini, J. Gauss and C. Puzzarini, *J. Chem. Theory Comput.*, 2018, 14, 5360–5371.
- 95 J. Liévin, J. Demaison, M. Herman, A. Fayt and C. Puzzarini, *J. Chem. Phys.*, 2011, 134, 064119.
- 96 J. Gauss and C. Puzzarini, *Mol. Phys.*, 2010, 108, 269–277.
- 97 C. Puzzarini and J. Gauss, *Mol. Phys.*, 2013, 111, 2204–2210.
- 98 G. Cazzoli, C. Puzzarini and J. Gauss, *Mol. Phys.*, 2012, 110, 2359–2369.
- 99 V. Barone, M. Biczysko, J. Bloino, F. Egidi and C. Puzzarini, *J. Chem. Phys.*, 2013, 138, 234303.
- 100 F. Pawłowski, P. Jørgensen, J. Olsen, F. Hegelund, T. Helgaker, J. Gauss, K. L. Bak and J. F. Stanton, *J. Chem. Phys.*, 2002, 116, 6482–6496.
- 101 P. Botschwina, *Phys. Chem. Chem. Phys.*, 2003, 5, 3337–3348.
- 102 S. Thorwirth, L. A. Mück, J. Gauss, F. Tamassia, V. Lattanzi and M. C. McCarthy, *J. Phys. Chem. Lett.*, 2011, 2, 1228.
- 103 M. Piccardo, E. Penocchio, C. Puzzarini, M. Biczysko and V. Barone, *J. Phys. Chem. A*, 2015, 119, 2058–2082.
- 104 E. Penocchio, M. Piccardo and V. Barone, *J. Chem. Theory Comput.*, 2015, 11, 4689–4707.
- 105 V. Barone, M. Biczysko, J. Bloino, P. Cimino, E. Penocchio and C. Puzzarini, *J. Chem. Theory Comput.*, 2015, 11, 4342–4363.
- 106 A. D. Becke, *J. Chem. Phys.*, 1993, 98, 5648–5652.
- 107 C. Lee, W. Yang and R. G. Parr, *Phys. Rev. B*, 1988, 37, 785–789.
- 108 V. Barone, *Chem. Phys. Lett.*, 1994, 226, 392–398.
- 109 S. Grimme, *J. Chem. Phys.*, 2006, 124, 034108.
- 110 M. Biczysko, P. Panek, G. Scalmani, J. Bloino and V. Barone, *J. Chem. Theory Comput.*, 2010, 6, 2115–2125.
- 111 S. Grimme, J. Antony, S. Ehrlich and H. Krieg, *J. Chem. Phys.*, 2010, 132, 154104.
- 112 C. Puzzarini, M. Biczysko, J. Bloino and V. Barone, *Astrophys. J.*, 2014, 785, 107.
- 113 M. C. McCarthy, V. Lattanzi, O. Martinez, J. Gauss and S. Thorwirth, *J. Phys. Chem. Lett.*, 2013, 4, 4074–4079.
- 114 M. C. McCarthy and J. Gauss, *J. Phys. Chem. Lett.*, 2016, 7, 1895–1900.
- 115 O. Zingsheim, M.-A. Martin-Drumel, S. Thorwirth, S. Schlemmer, C. A. Gottlieb, J. Gauss and M. C. McCarthy, *J. Phys. Chem. Lett.*, 2017, 8, 3776–3781.
- 116 B. Chandramouli, S. Del Galdo, M. Fusé, V. Barone and G. Mancini, *Phys. Chem. Chem. Phys.*, 2019, 21, 19921–19934.
- 117 G. G. Brown, B. C. Dian, K. O. Douglass, S. M. Geyer, S. T. Shipman and B. H. Pate, *Rev. Sci. Instrum.*, 2008, 79, 053103.
- 118 *Handbook of High-resolution Spectroscopy*, ed. M. Quack and F. Merkt, John Wiley and Sons, 2011.
- 119 J. C. Pearson, B. J. Drouin, A. Maestrini, I. Mehdi, J. Ward, R. H. Lin, S. Yu, J. J. Gill, B. Thomas, C. Lee, G. Chattopadhyay, E. Schlecht, F. W. Maiwald, P. F. Goldsmith and P. Siegel, *Rev. Sci. Instrum.*, 2011, 82, 093105.
- 120 D. T. Petkie, T. M. Goyette, R. P. A. Bettens, S. Belov, S. Albert, P. Helminger and F. C. De Lucia, *Rev. Sci. Instrum.*, 1997, 69, 1675–1683.
- 121 Z. Kisiel, O. Dorosh, M. Winniewisser, M. Behnke, I. R. Medvedev and F. C. De Lucia, *J. Mol. Spectrosc.*, 2007, 246, 39–56.
- 122 C. Puzzarini, G. Cazzoli and J. Gauss, *J. Chem. Phys.*, 2012, 137, 154311.
- 123 A. L. Steber, B. J. Harris, J. L. Neill and B. H. Pate, *J. Mol. Spectrosc.*, 2012, 280, 3.
- 124 G. B. Park, A. H. Steeves, K. Kuyanov-Prozument, J. L. Neill and R. W. Field, *J. Chem. Phys.*, 2011, 135, 024202.
- 125 G. G. Brown, B. C. Dian, K. O. Douglass, S. M. Geyer, S. T. Shipman and B. H. Pate, *Rev. Sci. Instrum.*, 2008, 79, 053103.
- 126 V. Wakelam, J.-C. Loison, E. Herbst, B. Pavone, A. Bergeat, K. Béroff, M. Chabot, A. Faure, D. Galli, W. D. Geppert, D. Gerlich, P. Gratier, N. Harada, K. M. Hickson, P. Honvault, S. J. Klippenstein, S. D. L. Picard, G. Nyman, M. Ruaud, S. Schlemmer, I. R. Sims, D. Talbi, J. Tennyson and R. Wester, *Astrophys. J. Suppl. Ser.*, 2015, 217, 20.
- 127 J. A. Montgomery Jr., M. J. Frisch, J. W. Ochterski and G. A. Petersson, *J. Chem. Phys.*, 1999, 110, 2822–2827.
- 128 J. A. Montgomery Jr., M. J. Frisch, J. W. Ochterski and G. A. Petersson, *J. Chem. Phys.*, 2000, 112, 6532–6542.
- 129 E. Papajak, J. Zheng, X. Xu, H. R. Leverentz and D. G. Truhlar, *J. Chem. Theory Comput.*, 2011, 7, 3027–3034.
- 130 S. Grimme, S. Ehrlich and L. Goerigk, *J. Comput. Chem.*, 2011, 32, 1456–1465.
- 131 C. Puzzarini and V. Barone, *Acc. Chem. Res.*, 2018, 51, 548–556.
- 132 D. A. Dixon, D. Feller and K. A. Peterson, *Ann. Rep. Comput. Chem.*, 2012, 8, 1–28.
- 133 Y. J. Bomble, J. Vázquez, M. Kállay, C. Michauk, P. G. Szalay, A. G. Császár, J. Gauss and J. F. Stanton, *J. Chem. Phys.*, 2006, 125, 064108.
- 134 M. E. Harding, J. Vázquez, B. Ruscic, A. K. Wilson, J. Gauss

- and J. F. Stanton, *J. Chem. Phys.*, 2008, 128, 114111.
- 135 T. Helgaker, W. Klopper, H. Koch and J. Noga, *J. Chem. Phys.*, 1997, 106, 9639.
 - 136 T. H. Dunning Jr., *J. Chem. Phys.*, 1989, 90, 1007–1023.
 - 137 D. E. Woon and T. H. Dunning Jr., *J. Chem. Phys.*, 1995, 103, 4572.
 - 138 J. Noga and R. J. Bartlett, *J. Chem. Phys.*, 1987, 86, 7041–7050.
 - 139 G. E. Scuseria and H. F. Schaefer III, *Chem. Phys. Lett.*, 1988, 152, 382–386.
 - 140 J. D. Watts and R. J. Bartlett, *J. Chem. Phys.*, 1990, 93, 6104–6105.
 - 141 M. Kállay and P. R. Surján, *J. Chem. Phys.*, 2001, 115, 2945–2954.
 - 142 Y. J. Bomble, J. F. Stanton, M. Kállay and J. Gauss, *J. Chem. Phys.*, 2005, 123, 054101.
 - 143 M. Kállay and J. Gauss, *J. Chem. Phys.*, 2005, 123, 214105.
 - 144 M. Kállay and J. Gauss, *J. Chem. Phys.*, 2008, 129, 144101.
 - 145 H. Sellers and P. Pulay, *Chem. Phys. Lett.*, 1984, 103, 463.
 - 146 N. C. Handy, Y. Yamaguchi and H. F. Schaefer, *J. Chem. Phys.*, 1986, 84, 4481.
 - 147 N. C. Handy and A. M. Lee, *Chem. Phys. Lett.*, 1996, 252, 425.
 - 148 W. Kutzelnigg, *Mol. Phys.*, 1997, 90, 909.
 - 149 R. D. Cowan and M. Griffin, *J. Opt. Soc. Am.*, 1976, 66, 1010.
 - 150 R. L. Martin, *J. Phys. Chem.*, 1983, 87, 750.
 - 151 A. Kendall, T. H. Dunning Jr. and R. J. Harrison, *J. Chem. Phys.*, 1992, 96, 6796.
 - 152 C. Puzzarini, M. Biczysko, V. Barone, L. Largo, I. Peña, C. Cabezas and J. L. Alonso, *J. Phys. Chem. Lett.*, 2014, 5, 534–540.
 - 153 S. Alessandrini, V. Barone and C. Puzzarini, *J. Chem. Theory Comput.*, 2020, 16, 988–1006.
 - 154 C. Puzzarini and V. Barone, *J. Chem. Phys.*, 2008, 129, 084306.
 - 155 V. Barone and P. Cimino, *Chem. Phys. Lett.*, 2008, 454, 139–143.
 - 156 A. S. Menon and L. Radom, *J. Phys. Chem. A*, 2008, 112, 13225–13230.
 - 157 J. Bloino, M. Biczysko and V. Barone, *J. Chem. Theory Comput.*, 2012, 8, 1015–1036.
 - 158 A. Baiardi, J. Bloino and V. Barone, *J. Chem. Theory Comput.*, 2017, 13, 2804–2822.
 - 159 D. E. Woon, *Astrophys. J. Lett.*, 2002, 571, L177.
 - 160 J. E. Elsila, J. P. Dworkin, M. P. Bernstein, M. P. Martin and S. A. Sandford, *Astrophys. J.*, 2007, 660, 911.
 - 161 R. A. Loomis, D. P. Zaleski, A. L. Steber, J. L. Neill, M. T. Muckle, B. J. Harris, J. M. Hollis, P. R. Jewell, V. Lattanzi, F. J. Lovas, O. Martinez, M. C. McCarthy, A. J. Remijan, B. H. Pate and J. F. Corby, *Astrophys. J. Lett.*, 2013, 765, 7.
 - 162 D. Quan, E. Herbst, J. F. Corby, A. Durr and G. Hassel, *Astrophys. J.*, 2016, 824, 14.
 - 163 R. D. Brown, P. D. Godfrey and D. A. Winkler, *Austr. J. Chem.*, 1980, 33, 1–7.
 - 164 F. J. Lovas, R. D. Suenram, D. R. Johnson, F. O. Clark and E. Tiemann, *J. Chem. Phys.*, 1980, 72, 4964–4972.
 - 165 M. Melosso, A. Melli, L. Spada, Y. Zheng, J. Chen, M. Li, T. Lu, G. Feng, Q. Gou, L. Dore, V. Barone and C. Puzzarini, *J. Phys. Chem. A*, 2020, 0, in press; doi: 10.1021/acs.jpca.9b11767.
 - 166 A. Belloche, R. T. Garrod, H. S. P. Müller, K. M. Menten, C. Comito and P. Schilke, *Astron. Astrophys.*, 2009, 499, 215–232.
 - 167 G. Wlodarczak, L. Martinache, J. Demaison, K.-M. Marstokk and H. Møllendal, *J. Mol. Spectrosc.*, 1988, 127, 178–185.
 - 168 H. S. P. Müller, A. Coutens, A. Walters, J.-U. Grabow and S. Schlemmer, *J. Mol. Spectrosc.*, 2011, 267, 100–107.
 - 169 S. C. Mehrotra, L. L. Griffin, C. O. Britt and J. E. Boggs, *J. Mol. Spectrosc.*, 1977, 64, 244–251.
 - 170 A. Belloche, R. T. Garrod, H. S. P. Müller, K. M. Menten, C. Comito and P. Schilke, *Astron. Astrophys.*, 2009, 499, 215–232.
 - 171 E. G. Bøgelund, B. A. McGuire, M. R. Hogerheijde, E. F. van Dishoeck and N. F. W. Ligterink, *Astron. Astrophys.*, 2019, 624, A82.
 - 172 A. J. Apponi, M. Sun, D. T. Halfen, L. M. Ziurys and H. S. P. Muller, *Astrophys. J.*, 2008, 673, 1240–1248.
 - 173 Z. Kisiel, A. Krasnicki, I. R. Medvedev, C. Neese, S. Fortman, M. Winnewisser, F. C. De Lucia and H. S. P. Muller, *ROTATIONAL SPECTROSCOPY OF ETHYLAMINE INTO THE THz*, 2009, 64th OSU International Symposium on Molecular Spectroscopy, TC-09.
 - 174 *Double and triple- ζ basis sets of the SNS family are available in the Download section*, <http://smart.sns.it/>, (last visited: 3 February 2019).
 - 175 C. Puzzarini, *J. Phys. Chem. A*, 2015, 119, 11614–11622.
 - 176 S. Zeng, I. Jiménez-Serra, V. M. Rivilla, S. Martín, J. Martín-Pintado, M. A. Requena-Torres, J. Armijos-Abendaño, D. Riquelme and R. Aladro, *Mon. Not. R. Astron. Soc.*, 2018, 478, 2962–2975.
 - 177 *Formamide*, <https://cdms.astro.uni-koeln.de/classic/molecules:ism:formamid>, (last visited: 12 January 2020).
 - 178 R. Saladino, G. Botta, S. Pino, G. Costanzo and E. Di Mauro, *Chem. Soc. Rev.*, 2012, 41, 5526–5565.
 - 179 R. Saladino, E. Carota, G. Botta, M. Kapralov, G. N. Timoshenko, A. Y. Rozanov, E. Krasavin and E. Di Mauro, *Proc. Natl. Acad. Sci.*, 2015, 112, E2746–E2755.
 - 180 E. F. van Dishoeck, *Faraday Discuss.*, 2014, 168, 9–47.
 - 181 C. Kahane, C. Ceccarelli, A. Faure and E. Caux, *Astrophys. J.*, 2013, 763, L38.
 - 182 A. Rimola, D. Skouteris, N. Balucani, C. Ceccarelli, J. Enrique-Romero, V. Taquet and P. Ugliengo, *ACS Earth Space Chem.*, 2018, 2, 720–734.
 - 183 V. Barone, C. Latouche, D. Skouteris, F. Vazart, N. Balucani, C. Ceccarelli and B. Lefloch, *Mon. Not. R. Astron. Soc. Lett.*, 2015, 453, L31.

- 184 C. Vastel, C. Ceccarelli, B. Lefloch and R. Bachiller, *Astrophys. J.*, 2014, 795, L2.
- 185 D. Licari, M. Fusè, A. Salvadori, N. Tasinato, M. Mendolicchio, G. Mancini and V. Barone, *Phys. Chem. Chem. Phys.*, 2018, 20, 26034–26052.
- 186 A. Pezzella, L. Panzella, O. Crescenzi, A. Napolitano, S. Navaratman, R. Edge, E. J. Land, V. Barone and M. d'Ischia, *J. Am. Chem. Soc.*, 2006, 128, 15490–15498.
- 187 G. Costanzo, A. Giorgi, A. Scipioni, A. M. Timperio, C. Mancone, M. Tripodi, M. Kapralov, E. Krasavin, H. Kruse, J. Sponer, J. E. Sponer, V. Ranc, M. Otyepka, S. Pino and E. Di Mauro, *ChemBioChem*, 2017, 18, 1535–1543.
- 188 M. d'Ischia, P. Manini, M. Moracci, R. Saladino, V. Ball, H. Thissen, R. A. Evans, C. Puzzarini and V. Barone, *Int. J. Mol. Sci.*, 2019, 20, 4079.